Fly ash from coal combustion - characterization

Aleksandra Stoch

Thesis to obtain the Master of Science Degree in

Energy Engineering and Management

Supervisors: Prof. Maria de Fátima Grilo da Costa Montemor
Dr hab. inż. Konrad Świerczek, Prof. AGH

Examination Committee

Chairperson: Prof. José Alberto Caiado Falcão de Campos
Supervisor: Prof. Maria de Fátima Grilo da Costa Montemor
Members of the Committee: Prof. Rui Duarte Neves
Prof. Mário Manuel Gonçalves da Costa

February 2015

Acknowledgments

This thesis is based on the work conducted within the KIC InnoEnergy Master School, in the MSc programme Clean Coal Technologies. This programme is supported financially by the KIC InnoEnergy. The author also received financial support from KIC InnoEnergy, which is gratefully acknowledged.

KIC InnoEnergy is a company supported by the European Institute of Innovation and Technology (EIT), and has the mission of delivering commercial products and services, new businesses, innovators and entrepreneurs in the field of sustainable energy through the integration of higher education, research, entrepreneurs and business companies. Shareholders in KIC InnoEnergy are leading industries, research centres, universities and business schools from across Europe.

The MSc programme Clean Coal Technologies is a collaboration of:

AGH University of Science and Technology, Kraków, Poland,

SUT Silesian University of Technology, Gliwice, Poland

IST Instituto Superior Técnico, Lisbon, Portugal

Acknowledgments

I would like to express my great thanks and appreciation for valuable advices and constructive comments that I received from Prof. Fátima Montemor, my supervisor at Instituto Superior Técnico (IST). I am also thankful for her time and dedication, as well as, for a very pleasant and effective cooperation.

I would like to express my deep gratitude for help with research and results interpretation to dr hab. inż. Konrad Świerczek, Prof. AGH, my supervisor at University of Science and Technology (AGH). I am grateful for his willingness to give his time and his dependable scientific support.

Additionally, I would like to thank you all, who have contributed to the creation and completion of this dissertation.

At the end, I wish to give thanks to my reliable family and my beloved fiance, who support me mentally during the entire process of creating this work.

This dissertation was made in cooperation with *EDF* (Polska S.A. R&D Center located in Kraków (Poland), which provided samples of ashes to analyze coming from one of EDF Polska S.A. coal fired boilers as well as information regarding the power plant operation.

Abstract

Combustion is a well-known process used in power plants and combined heat and power plants to obtain electricity and optionally also heat from the fuel. During combustion of coal, besides the desired electrical energy some byproducts are also produced. The most abundant byproduct of coal combustion is fly ash.

Fly ashes (FA) are fine, grey particles or powders, which are considered environmental pollutants. FA particles from the power plants are captured via electrostatic precipitators (ESPs). Moreover fly ash properties depend upon the origin of the fuel and parameters used during the combustion process. Therefore it is crucial to details the characteristics and properties of fly ash, prior to use fly ash particles in any application.

Thus this MSc. Dissertation project aims at characterizing fly ash in terms of morphology using scanning electron microscopy (SEM), elemental composition using Energy dispersive X-ray analysis (EDX) and phase composition using X-ray diffraction (XRD). The fly ash samples were divided into five fractions with fly ash diameter sizes: under 63 µm, 63-100 µm, 100-200 µm, 200-320 µm and above 320 µm. This separation aimed finding a tendency between the size of fly ash particles and their morphological and structural properties, elemental composition and phase composition. Furthermore, fly ash particles were also submitted to size range measurements using a Malvern Mastersizer 2000 instrument, which provided detailed information about the amount of individual particles in weight percentage.

The results indicate that the morphology of the different fractions shows significant differences. The elemental composition of the individual fractions depends on the particles size and it was observed that, some elements such as P, Mg, S, Fe, Cu were the ones, evidencing the more marked dependencies.

Keywords: Fly ash, coal combustion, size distribution, elemental composition

Resumo

A combustão é um processo industrial muito bem conhecido, que é utilizado em centrais de produção de energia e instalações de cogeração, visando a produção de electricidade e também de calor. Durante a combustão do carvão são produzidos vários subprodutos de entre os quais se destacam as cinzas volantes.

As cinzas volantes (FA), são partículas finas que são consideradas como poluentes, constitutindo um problema ambiental. As cinzas volantes produzidas em centrais termoelétricas são capturados por precipitadores eletrostáticos (ESPs). É bem conhecido que a composição e as propriedades das, cinzas volantes dependem da origem do combustível processado também de parâmetros inerentes ao processo de combustão. É da maior relevância conhecer em detalhe as propriedades e a composição das cinzas volantes com vista a potenciar a sua utilização em aplicações diversas. O Objectivo final é que este subprodutopossa ser consumido de forma sustentável.

Assim, o objetivo deste trabalho consiste na caracterização detalhada das cinzas. Para o efeito utilizou-se a microscopia eletrónica de varrimento (SEM) de modo a conhecer a morfologia, análise química elementar (EDX) e ainda a difração de raios-X (DRX) com vista à deteção de fases cristalinas. Para o efeito as cinzas volantes foram divididas em cinco fracções, com diâmetros caracteristicos correspondentes a: inferior a 63 microns, 63-100 microns, 100-200 microns, 200-320 microns e, acima de 320 microns. Esta separação visou encontrarcorrelações entre o tamanho de partículas e as s propriedades morfológicas, estruturais e composição elementar das cinzas volantes. As cinzas volantes foram também sujeitas a medidas para determinação do tamanho de partícula, utilizando o equipamento Malvern Mastersizer. Este equipamento permite quantificar as amostras em termos de percentagens de peso.

Os resultados evidenciaram que a morfologia das diferentes frações era bastante distinta. Por outro lado verificou-se também que a composição elementar das fracções individuais também era bastante sensível ao tamanho de partícula. Alguns elementos, como P, Mg, S, Fe, Cu evidenciaram tendências dependentes do tamanho de partícula.

Palavras-chave: cinzas, a combustão do carvão, distribuição de tamanho, composição elementar

Content

List of Tables

List of Figures

Introduction

Presently, electricity and heat are essential for the development and functioning of the modern civilization. Through the years, an increased demand for electrical energy has been recorded. The world's production of electricity is still greatly based on the thermal conversion of solid fossil fuels, which produces a number of wastes. Annually, the energy sector uses approximately $3.5 \cdot 10^9$ tonnes of coal, which allows to produce about 38% of the world's electricity [1].

Wastes are all the by-products produced during the combustion processes. The combustion of coal originates various types of by-products and among these, fly ashes are the most abundant. Typically fly ashes distribution includes the fly ash (70 - 90%) and the bottom ash (10 – 20%). Other coal combustion by-products include boiler slag, flue gas desulphurisation, gypsum or other types of materials such as fluidised bed combustion ashes, cenospheres and scrubber residues. Figure 1 shows the by-products distribution and their production situated on lay out of the coal combustion process.

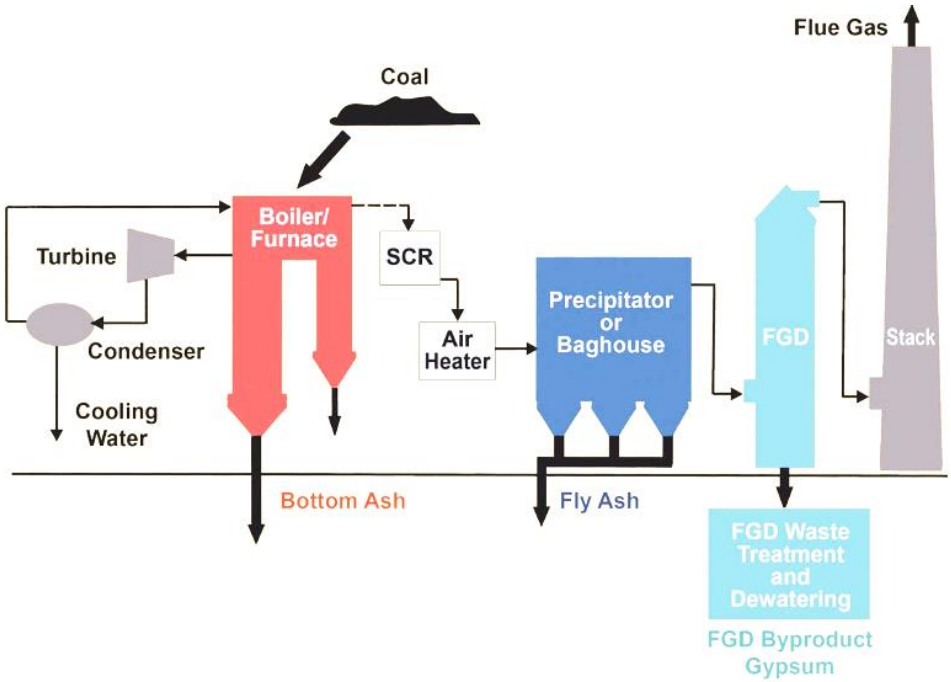

Figure 1 Coal combustion by-products distribution [2].

In recent years, the power industry underwent a series of transformations, leading to significant technological and efficiency improvements. The actual targets of the sector aim at reducing the cost of energy production, optimizing the use of fuel as well as reducing the impact of power plants on the environment. Therefore, new technologies are being introduced and existing ones have been improved. For example, in power plants, there is a trend to replace pulverized boilers by fluidizing bed boilers. Many plants also installed desulphurization and denitrification systems. In addition, the composition of the fuel changes, as well as the composition of bituminous coal and lignite. Moreover there is an increase of energy production from biomass. Therefore, the composition and properties of wastes changes and, in particular those referring to fly ash are essential to be known [23].

Fly ashes are mineral residues from coal combustion that leave the furnace together with the flue gases. Thereafter fly ash particles are captured using dust collection equipment, mainly electrostatic precipitators. It is estimated in the world, that each year, the production of fly ash is around $4.2 \cdot 10^8$ tonnes of fly ash – mostly in China and United States, while in Poland it is approximately $4.2 \cdot 10^6$ tonnes of fly ash (2009). Fly ash physical, chemical and mineralogical properties combined with its large scale production make fly ash an attractive raw material for various applications. Therefore, in order to promote the usage of waste fly ashes, it is essential to study and to characterise in deep this material. This will allow its widespread use as raw materials in many areas of the economy [1]. Thus, the objective of this dissertation is to characterize various fractions of fly ash and in particular to detail its size distribution and chemical composition.

1. Coal

In general coal is an organic, non-renewable fuel with more than 50% by weight of carbonaceous material. It is a complex combustible sedimentary rock, mostly derived and composed of plant debris and metamorphosed plant derivatives. Primarily deposited as a peat or mud, is transformed to coal by physical and chemical processes. The transformation is caused by compaction and heat during long-term embedding in depths up to several kilometres and periods longer than few hundred millions years. Coal properties and composition depend upon the original plant materials and their extent of decay [4, 50].

Hence, coal composition can vary significantly. Typical ranges for fixed carbon, moisture, ash and sulphur contents for different types of coal are presented in Table 1. The most important part of the coal is fixed carbon which relative content increases from 30 wt.% in lignite coal to 85 wt.% in anthracite. However, the most important coal from the view point of this work is the bituminous one.

Table 1 Composition of various types of coal in wt.% [3].

Type of Coal	**Fixed Carbon**	**Moisture**	**Ash**	**Sulphur**
Lignite	31.4	39	4.2	0.4
Bituminous	44.9 – 78.2	2.2 – 15.9	3.3 – 11.7	0.7 – 4.0
Anthracite	80.5 – 85.7	2.8 – 16.3	9.7 – 20.2	0.6 – 0.77

Worldwide coal is the most frequently used organic fuel in energy production. Despite the fact that the use of coal has a direct impact on climate change and human health, the trend of using this fuel has been rising during the years due to increased energy demand. In 2006, coal constituted 25% of primary energy supply in the world. The world situation can be summarized as follows: in 2006 China was the largest consumer of coal, constituting for 39% of global coal consumption, USA accounted for 18%, European Union 10% and India 8% [38].

Naturally, extraction of energy from the coal is performed by combustion. The precise description of this process is presented in chapter of *Technology related to fly ash production*. The coal combustion process is described considering the type of industrial boiler i.e. pulverized coal fired boiler and fluidized bed boiler.

1.1. Inorganic Components

Generally, the inorganic elements in coal are transformed into ash during the process of combustion. Ash formation depends on various parameters but it is strictly hinge on quantity and quality of inorganic matter. The inorganic elements of coal have been referred as mineral matter, minerals, inherent or extraneous ash etc.

The inorganic elements from coal occur as discrete minerals, amorphous phases, organically associated cations, and cations dissolved in pore water. The fractions originally associated to the inorganic components differ significantly, depending on the coal rank. Also there are differences in the content of oxygen: for example lower-ranked subbituminous coals or lignite possess higher levels of oxygen. Around 25% of the oxygen is in the carboxylic acid group form. These groups have special roles since they behave as bonding sites for cations such as sodium, calcium, magnesium, potassium, strontium and barium. The origin of these cations is specific of the original plant material, which constitutes the first stage of coal and from the groundwater filtering through the coal. In several low-rank coals content of the originally associated inorganic components amount 60% of total inorganic content in the coal [5]. In higher-ranked coals, such as bituminous and anthracite, the inorganic components consist largely of minerals.

The richest components in coals are usually mineral grains. The major mineral groups consist of silicates, oxides, carbonates, sulfides, sulfates and phosphates. Another main group of minerals in coals are the so-called detrital minerals. These minerals were transported by water and wind during the early stages of coalification. The detrital mineral group include silicates hence clay minerals and quartz. Such minerals, formed during the prime stage of coalification or coal beds deposition are called syngenetic. Components of syngenetic minerals are carbonates, sulfides, oxides and phosphates. Also there are epigenetic minerals formed during the later stages of coalification. These minerals consist mainly of carbonates, sulfides and oxides that were created in fissures or cleats. The fundamental differences between epigenetic and syngenetic minerals is that epigenetic minerals are more likely to be mixed with the organic coal minerals because of the original route of its formation.

To be able to predict the behaviour of the inorganic components during process of combustion, it is necessary to obtain information about quantity, size and association of mineral matters in the coal. The association of mineral grains needs to be known and classified. In addition, there is a division depending upon the association of the organic part. If a mineral is associated with the organic part then it is called included; when it is not associated with the organic part it is considered to be excluded. There is also another term which present the association of the minerals; it is juxtaposition that is related to the general

minerals association with coal and with other minerals [6]. For instance, an individual particle of coal may include minerals as quartz, kaolinite and pyrite. Figure 2 illustrates information about coal and associated inorganic components. This information is essential in modelling and predicting the evolutions in the composition and size of ash during coal combustion.

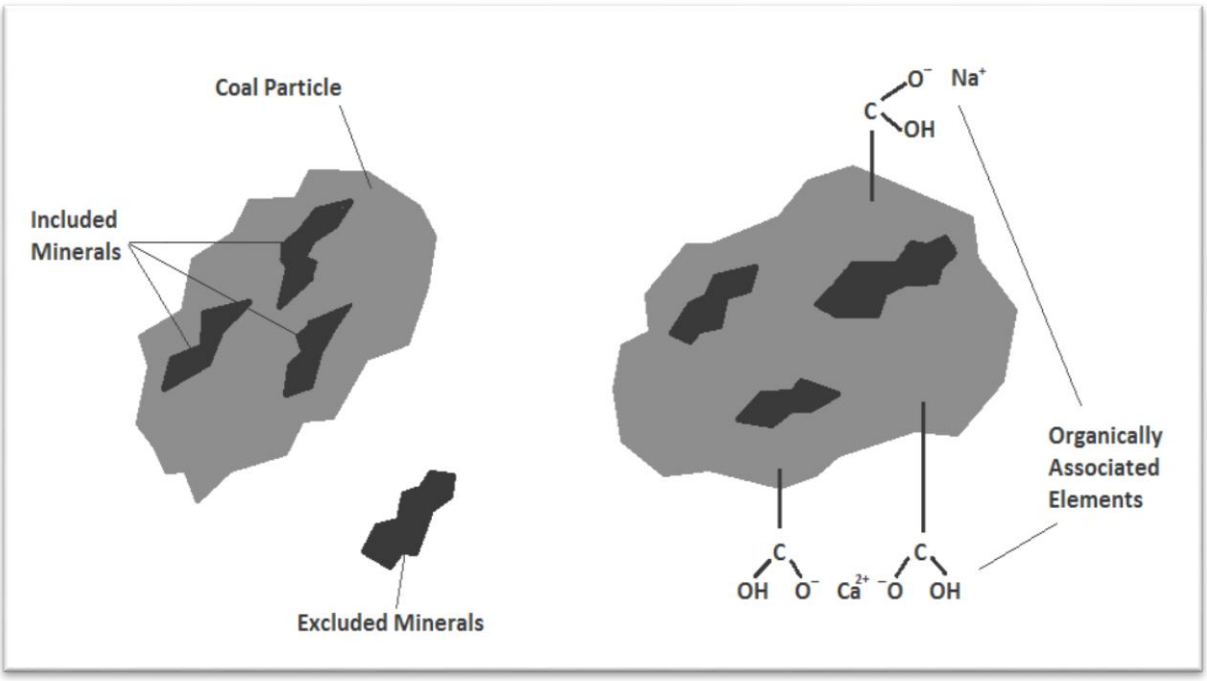

Figure 2 Inorganic components associated in coal [4].

There are various methods to determine the properties and composition of inorganic components in coal. Usually the standard methods provide a rough classification of inorganic components by ashing or gravity separation techniques. However these methods do not allow assessing quantitative information about inorganic associations and the amount of inorganic components. However, more advanced techniques such as computer-controlled scanning electron microscopy (CCSEM) and chemical fraction provide quantitative results that include composition, abundance, size and association of inorganic components in coals.

The transformation processes are complex in what concerns chemical and physical aspects. Quantity and quality of the ash precisely depends upon the type of coal, the combustion conditions of the process and of the content of inorganic matter. There are various methods based on composition of the coal, such as for example the ashing technique, which is able to predict the physic-chemical properties of the ash.

1.1.1. Physical Transformations

As stated above, the fly ash inorganic composition depends upon the coal and combustion conditions; the same dependence can be considered concerning the physical transformation of inorganic compounds in the coal. There are several possible combinations of inorganic components associated to coal particles. For example, mineral-mineral, mineral-coal, mineral-cation-coal and mineral-mineral-cation-coal, are all associated in coal. This association distinguishes coal and makes each coal sample unique. The various transformations that may occur during the coal combustion are illustrated on Figure 3.

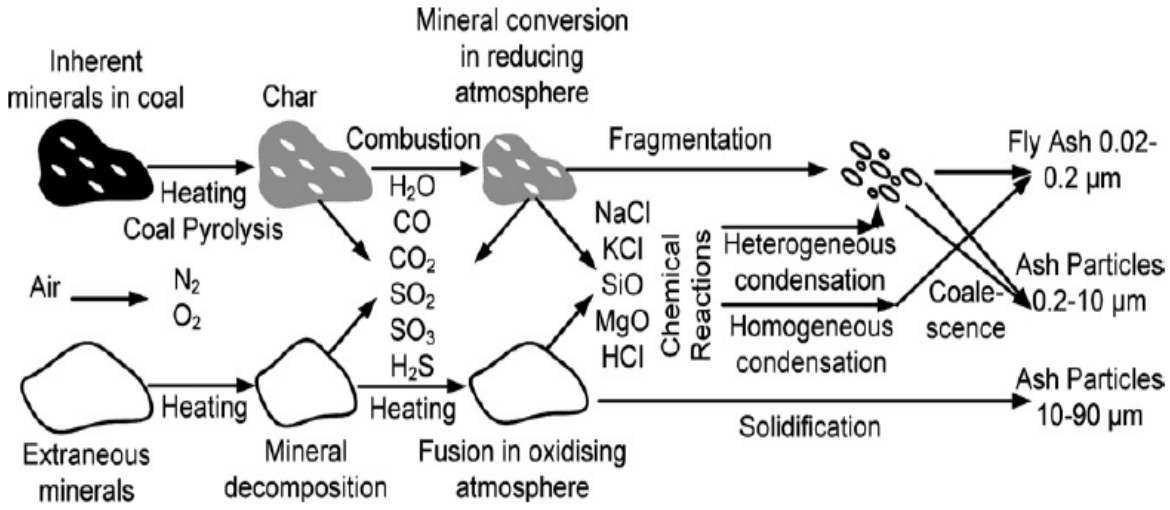

Figure 3 Schematic diagram of coal fly ash formation [42].

As shown in Figure 3, several possible transformation include (a) coalescence of particular mineral grains within a char particle, (b) shedding of individual ash particles from the char surface, (c) disintegration of the char, which does not allow complete coalescence, (d) ash convective transport from the char surface over devolatilization, (e) fragmentation of particles of the inorganic components, (f) formation of the cenospheres and (g) evaporation and further condensation of the inorganic constituents upon gas cooling.

As an outcome of above interactions, the final form of ash is characterised by a bimodal size distribution which is illustrated in Figure 4. The submicron components are mostly products of the condensation of flame-volatilized inorganic constituent. The larger particles reach the mass diameter between 12 to 15 micrometers, but this depend upon the type of coal and conditions of the combustion. These larger particles have been referred as residual ash.

The transformation of excluded minerals depends on the physical characteristics of the mineral. Minerals which are excluded, like quartz (SiO2), after passing through the combustion system still show the same untouched angular structure. The excluded minerals, like clays, can be fragmented under dehydration and can melt to form cenospheres, while the excluded pyrite behaviour depends on its morphology. Sometimes the pyrite may occur as framboids, which can produce fragments more easily.

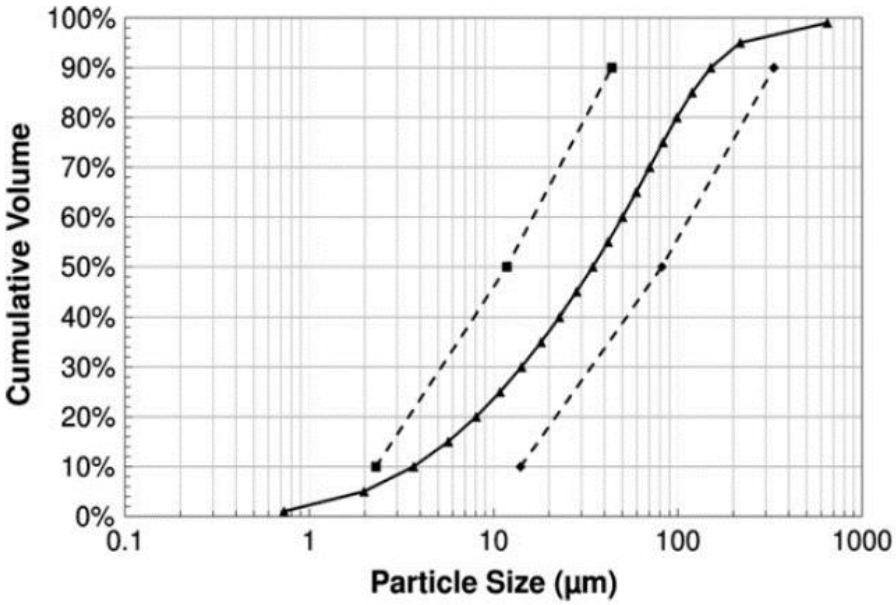

Figure 4 Typical fly ash size distribution with upper and lower ranges [35].

The transformations of the included minerals can be correlated to the combustion characteristics of the char particle. It is essential to consider two stages of the coal combustion process which consist of (i) rapid devolatilization and (ii) char combustion. During the first combustion stage, the coal particles are heated-up and proceed to the pyrolysis process, leading to release, ignition and volatile combustion; the second stage of combustion is the oxidation of the char. Usually the two stages are sequential but they may also be simultaneous. The time to the overall process of combustion of pulverized coal particles is less than one second. The temperature of the process depends upon the percentage of the air excess, quality of coal, mixing of fuel and air, and particles sizes. The temperature of the combustion gases may accomplish 1810 K, and the temperature of burning char particle may reach 200-400 K. The non-volatile inorganic matter mostly remains with the char after combustion and only few ash particles might be found associated with the volatiles [27, 35].

1.1.2. Chemical Transformation

The discussion of the chemical transformations of inorganic matter requires to consider various chemical systems that consists of aluminosilicates, silicate, sulfate, phosphate, chloride and sulphide. There is also an important role played by iron, alkali and alkaline earth oxides.

The chemical composition influences the melting behaviour of the ash particles during combustion. The development of components of fly ash is illustrated at Figure 5. The figure shows that during the process of combustion transformation of minerals such as pyrite, aluminosilicates and K-aluminosilicates takes place. The outcomes of this transformation are iron oxides, iron aluminosilicates and other phases of glass complex. The particles of fly ash differ in size and chemical composition.

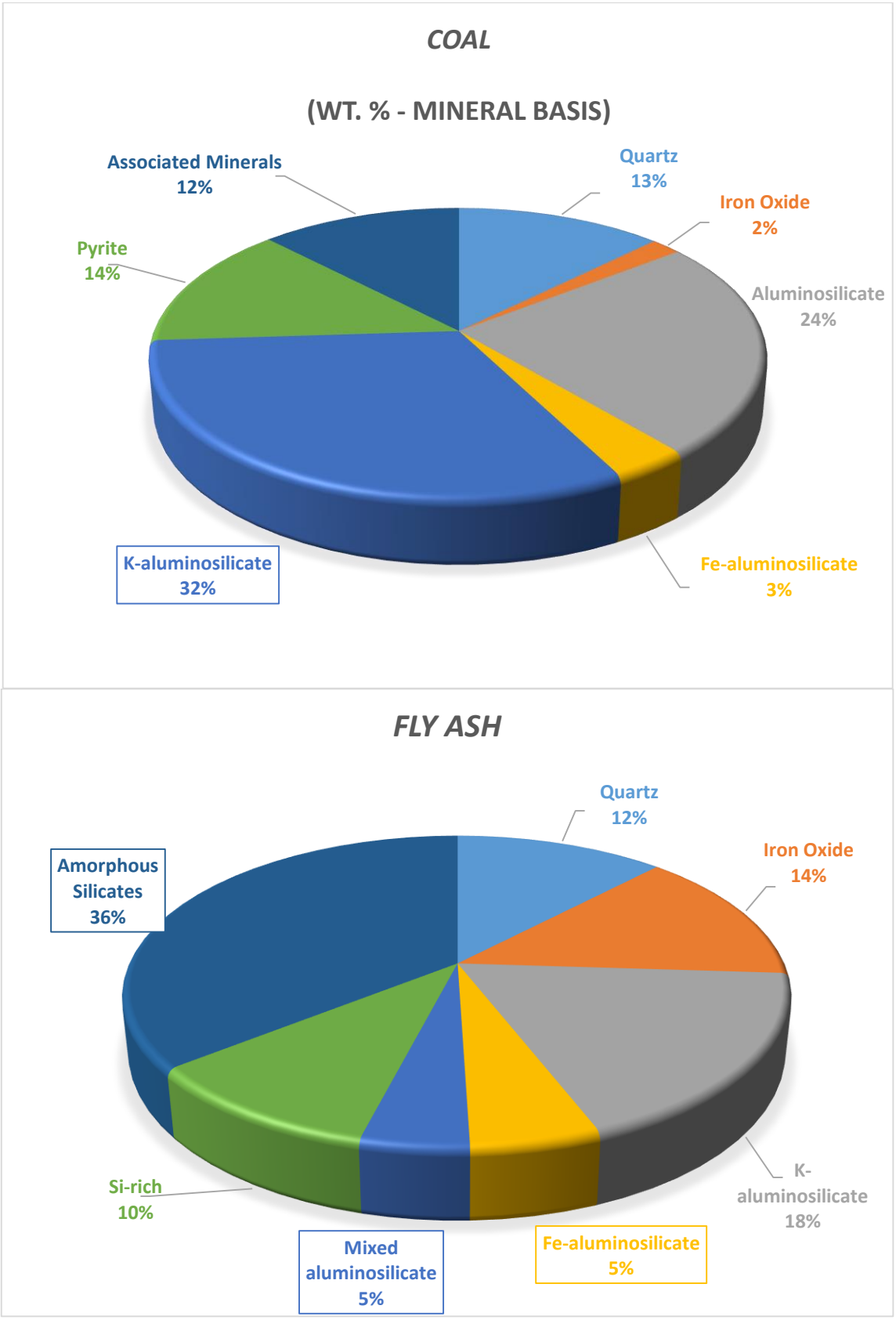

Figure 5 Evaluation of composition during combustion of bituminous coal ash (wt % mineral basis) upper coal composition, bottom fly ash composition [4].

Generally, fly ash obtained via pulverised coal combustion is 90-95% amorphous and mainly contains silicate glass. Glass is an inorganic product that can be quenched to hard conditions without crystallizing: it is in liquid form and has very high viscosity. Properties and phases of these glassy components are gaining importance especially in predicting ash deposition processes.

2. Technology related to fly ash production

Presently, worldwide there are plenty of technologies by which electricity can be produced. Besides electricity, industrial heat is also very important in countries characterised by low temperate climates such as Poland. In Poland, the dominant power plants are condensation power plants and combined heat and power plants (CHP). These power plants are mostly fired by coal, lignite and biomass. Condensation power plants and CHP power plants vary in the method applied for steam cooling and utilization of waste heat.

Condensation power plants make use of technology that allows the conversion of chemical energy of the fuel generated in the combustion process into thermal energy of steam, which in the process of thermal expansion in the turbine is converted to kinetic energy – mechanical energy. Then in the generator driven by a turbine, there is conversion of mechanical energy into electrical energy. The resulting electric energy is transformed to a high voltage and transferred to grid and then it is distributed to the final customers.

In contrast, CHP plants, apart from electrical energy, which is produced identically as in the condensing power plants, also produce heat energy in the form of water or steam. In this case, steam which is partially expanded in a steam turbine is directly used as technological steam or used to heat industrial water. Industrial water is circulated in a closed circuit and used in the municipal heating. Part of the water vapour, which is taken from the turbine, is not submitted to condensation in the condenser. This significantly reduces the losses of energy due to cooling water and that results in increased efficiency. Therefore the combined heat and power plants are more efficient compared to the condensing power plants [49].

In the aforementioned condensation and CHP plants, two different types of boilers are normally used: pulverized coal boilers or fluidized bed boilers provided with fixed bed or circulating bed. In power plants equipped with conventional pulverized coal boilers there is production of fly ash (conventional one without any additives) and fly ash with additional flue gas desulfurization products. Fly ashes, with addition products, are produced when dry or semi-dry methods of flue gas desulphurization are applied. On the other hand, fluidized fly ash is produced in power plants equipped with fluidized bed boilers.

The next section describes, in brief, the characteristics of the process of formation and release of fly ash from pulverized coal boilers (PC) and in fluidized bed boilers (FB).

2.1. Fluidized Bed Combustion

One class of boilers used in power plants are the fluidized bed boilers. Fluidized Bed Combustion **(FBC)** is a clean burning technology, in which directly in the combustion chamber there is a decrease of basic pollutants in the total emissions. In comparison to the pulverized coal boiler, the combustion chamber is smaller as a result of the intensity of combustion in the fluidized bed. This also affects the temperature of the combustion process, which is in the range of 800 – 900^{o}C. Furthermore, by lowering the temperature of the process, the generation of nitrogen oxides during combustion and oxidation of sodium and vanadium particles is reduced. Moreover, in fluidized bed boilers it is possible to use different types of fuel, including fuel with low-quality, lower calorific value and polluted fuel. Additionally, the combustion leads to a reduction of SO_2 emissions by bringing to the bed sulphur-binding compounds. Fluidized bed boilers can be divided into two main types: atmospheric fluidized bed combustion (AFBC) and pressurized fluidized bed combustion (PFBC). Both may exist in two versions: bubbling circulating bed (BFB) and the circulating fluidized bed (CFB) [30].

Similarly, as in the case of pulverized coal-fired boilers, the combustion process in the fluidized bed boilers is also a multistep process. In the first step pulverized fuel i.e. bituminous coal, lignite or biomass and sorbent (for example limestone $CaCO_3$, dolomite $CaCO_3 \cdot MgCO_3$) are entered into combustion chamber, where together with the inert material (i.e. sand, ash) form a bed. To ensure an adequate turbulence there is steady stream of air or oxygen blown into the fluidized bed, thereby achieving the condition of particles suspension in the gas stream. Grains of fuel are degassing in three stages. Firstly, fuel is heated to the softening temperature (350 - 480°C), then moisture is evaporated. Secondly, decomposition of the coal occurs and there is a transition to the plastic state with the simultaneous release of volatiles. As the temperature increases, larger amounts of liquid and gaseous decomposition products of coal are emitted, and coal grains form a semi-plastic mass, with appearance and behaviour that can be quite different, depending on the type of coal. Further increase in temperature (470 - 510°C) results in the semi-coke. In the third stage there is the complete degassing of semi-coke and therefore the transition to coke. Initially solidified semi-coke still emits volatiles, but the processes of polymerization and condensation of carbonaceous material begins. For temperatures around 700°C, the carbon residues are combusted and oxidation of pure carbon may occur, while the mineral part remains. At this point begins the process of creating fluidized fly ashes which are discarded from the bed with the flue gas. High fragmentation of semi-coke and coke is disadvantageous, because the smallest grains cannot be burned so they are moved out from the boiler with the ash. Continuous mixing in the bed improves the combustion efficiency of fuel and contributes to maintain constant temperature in the combustion zone. Simultaneously, with the combustion process, the flue gas desulfurization process takes place; it is formed during the combustion by binding sulphur through the bed [31, 32].

Fly ash from fluidized bed boilers as well as in the conventional ash, is separated from the flue gas stream in electrostatic precipitators. However, fluidized fly ash is significantly different from fly ash from pulverized boilers. Difference is due to lower combustion temperature and the use of limestone to neutralize the sulphur oxides in the fluidized bed. Hence, there is a difference in the morphology and phase composition. By-products of conventional coal combustion have potentially hazardous elements

on generally low level, but volatiles elements, which condense on the smallest fractions of fly ash are more dangerous. In case of by-products from fluidized bed combustion, volatile elements are less relevant because of lower pressure, but solid residues can be potentially hazardous elements on a more significant level [32].

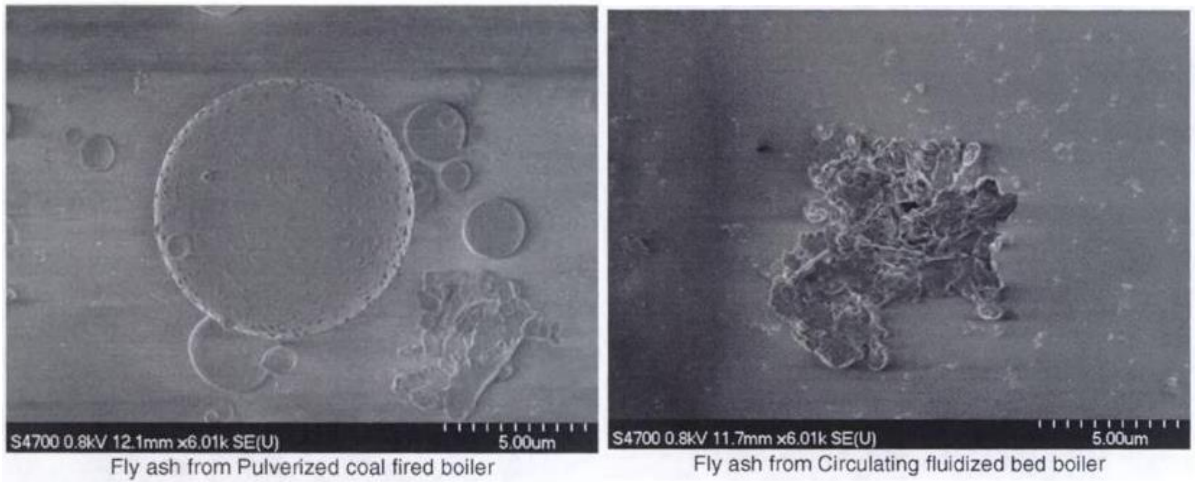

Figure 6 Scanning electron microscope photographs of sample of fly ash from pulverized coal-fired boiler and from circulating fluidized bed boiler [29].

The micrographs depicted in Figure 6 evidence some morphological differences. Fly ash from conventional combustion displays a spherical shape and particles from the fluidized bed combustion are characterized by irregular, sharp-edged shapes.

2.2. Pulverized Coal Combustion

In Pulverized Coal Combustion **(PCC)** coal is introduced via dust burners into the combustion chamber, where zones with maximum temperatures between 1450 – 1600^{o}C can be distinguished. These are known as 'flame core' zones of the combustion chamber. To achieve the desired efficiency pulverized coal is put into swirling motion around the flame core. However, there is a small amount of pulverized coal, which do not pass through the zone of maximum temperatures, thus these are not completely combusted. Despite the fact that temperature in the core of the furnace is greater than the melting point of most of the materials contained in coal there is still about 20-50% of materials that remain non-melted.

Combustion in pulverized coal-fired boilers is a multistage process. In the first stage for temperatures around 350^{o}C, water physically absorbed on the surface of fuel particles evaporates, and the initial release of the volatile components occurs. In the second stage, in temperature ranges between 350 – 600^{o}C, grains of coal soften, a process that promotes further release of volatiles. In this temperature loamy materials begin to undergo the process of dehydroxylation. In the next stage, which is characterised by temperatures above 600 ^{o}C, grains of coal come under thermally swell, there is completely devolatilization, and finally auto-ignition resulting in coke formation. These processes last only 0,01 - 0,2 seconds. In a subsequent step, coke residues are combusted, coal grains are disintegrated due to the oxidation of fuel and of remaining mineral matter. This stage lasts 0,5 – 5

seconds. Moreover, this step is also the starting one for the formation of fine and thick fractions which correspond, respectively, to particles of fly ash and sand slag. In this process highly dispersed mineral matter is melted, developing a spherical shape. Further degassing steps cause swelling of the majority of the resulting spheres and microspheres that are formed. Some by-products of combustion, such as slag accumulate under the grate in the bottom of the combustion chamber, while fly ash is removed with flue gases from the combustion chamber by fans [30].

2.3. Electrostatic Precipitators

The exhaust gases with suspended fly ash are subjected to dust extraction. Dust extraction takes place most frequently in electrostatic precipitators (ESPs) that are devices able to separate solid fine particles from a gas stream with efficiency up to 99,9%. An electrostatic precipitator comprises a compartment divided into three fields, two sections for each.

Generally, the principle of the operation is based on electrostatic attraction. Particles in the gas stream that are negatively charged migrate to the collecting electrodes. The collecting electrode is a positive charged grounded plate. The negative charging of the particles is caused by discharge electrodes which may have the form of wires spaced between plates. A negative high-voltage by direct current is applied to the wires to create the negative electric field. The voltage applied to the wire is increased until a corona, which is visible luminous blue glow around the wires is produced. The free electrons created by the corona escape from the negative electric field very rapidly. Because of the acceleration caused by the electrons that are liberated, gas molecules become positively charged, thus, becoming positive ions. All this electrons generation is called avalanche multiplication. The field can be conventionally divided into three regions. The discharge electrode region has the strongest field, and here the particle charging process is started. The weaker field can be found in the inter-electrode region, which is in the area between the discharge and the collection electrodes. The weakest field is found near to the collection electrode. After this fast operation, particles move to the positively charged collection electrodes, where they are gathered. When particles and dust deposit, collection plates and discharge electrodes may be rapped. Rappers impart a vibration to the electrodes, removing accumulated dust. Process must occur at the correct current intensity to guarantee that the proper amount of material is removed. Occasionally, water sprays can be used do remove dust from collection electrodes. Afterwards particles or dust, which are removed from the electrodes are transported by gravity into special bins called hoppers. Hoppers collect and temporary store the particles. They are located at the bottom of ESP [33, 34, 43, 44].

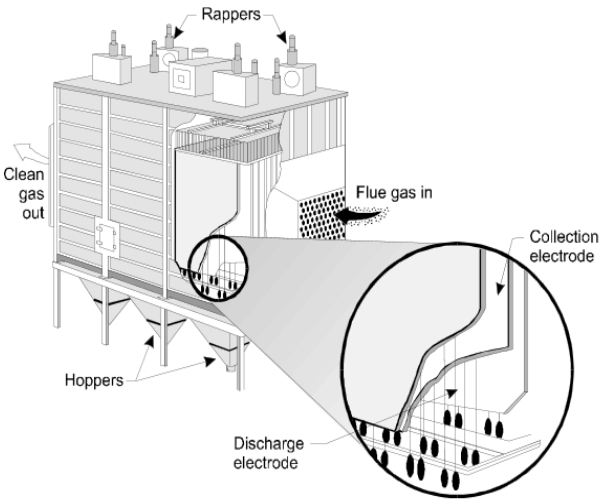

Figure 7 Schema of typical ESP [33].

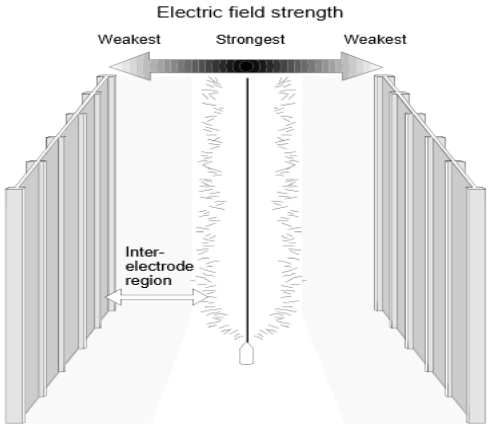

Figure 8 ESP electric field [33].

In addition, the ESP comprises three individual sectors, divided into two parts each, illustrated on Figure 9. By such treatments the efficiency of these types of dust removals is high. In all the sectors, particles are removed. The largest removal occurs in first sector most while in the second sector less particles are removed and, finally in third one only residual amounts are removed. From each sector particles or dust are removed through hoopers into storage reservoirs, from where they can be managed and collected.

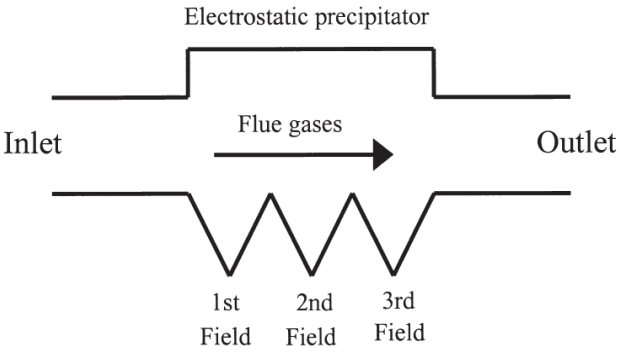

Figure 9 Collecting fields for fly ash in electrostatic precipitators [44].

3. Fly Ash

Fly ash (FA) are fine, grey particles or powders as it is shown in Figure 10. Fly ash can also be called flue-ash or coal fly ash (CFA) depending on the fuel of origin. Generally FA is generated during the process of coal combustion, being produced as a side product, waste. Also fly ash, being an industrial by-product is considered an environmental pollutant. Therefore, nowadays, fly ash, which leaves the furnace with flue gases is collected by electrostatic precipitators (or other equipment for example baghouse) and then fly ash can be utilized or landfilled.

Figure 10 Fly ash [41].

The environmental incentives encourage re-utilization of fly ash. Fortunately physical, chemical and mineralogical properties allows to fly ash utilization in a wide range of applications in many areas of the economy. The most important classifications, properties and applications are described in the next chapter.

3.1. Classification

First, it must be noted that there is no clear definition of the term ‘fly ash’, which is often the source of many misunderstandings concerning research in this particular field as well as in their use. There is also no consistent system of classification of fly ash. In addition, existing systems, very commonly relate only to a narrow range of application of fly ash wastes. Furthermore, each country has its own national classifications based on various sources such as legislation, standards, publications, etc.

Therefore, in this chapter the overall distribution of fly ash concerning their origin and hereby presented in accordance to the *American Society for Testing and Materials* ASTM C618-12.

Fly ashes are considered residues obtained after combustion of coal that do not remain in the combustion chamber but are expelled as suspended solid particles in the exhaust gases. They might be collected by the dust extraction equipment e.g. electrostatic precipitators or filter bags as described in the previous chapter.

Fly ash can be broadly categorized according to:

- furnace construction:
    - fly ash from the combustion in conventional boilers,
    - fly ash from the combustion in fluidized bed boilers,

- the type of fuel used in power boilers:
    - fly ash from bituminous coal combustion,
    - fly ash from bituminous coal and biomass combustion,
    - fly ash from lignite combustion,
    - fly ash from lignite and biomass combustion,

- selective method of collecting fly ash from different sections of electrostatic precipitators:
    - fly ash from zone I,
    - fly ash from zone II,
    - fly ash from zone III,

- flue gas desulphurization technology:
    - conventional fly ash,
    - conventional fly ash which contain flue gas desulphurization products,
    - fluidized fly ash

Fly ash can also be divided into siliceous fly ash and calcareous fly ash. The first mentioned siliceous fly ash mainly consist reactive silicon dioxide (SiO_2) and aluminium oxide (Al_2O_3); it also possesses pozzolanic properties. On the other hand, calcareous fly ash consists on reactive calcium oxide (CaO), reactive silicon dioxide (SiO_2) and aluminium oxide (Al_2O_3) and shows both pozzolanic and hydraulic properties [15, 28].

Meanwhile, different approaches to classify fly ash have been presented and often cited in the literature. This includes for example the American standard - ASTM C618-12. It classifies fly ash according to the type of coal, from which they are formed.
According to ASTM C618-12 the fly ash can be divided into:

- Class F fly ash,
- Class C fly ash.

Class F includes ash from the burning of bituminous coal. Ashes belonging to this class have pozzolanic properties. Class F consists mainly on siliceous fly ash.

Class C fly ash is produced from combustion of subbituminous coal and lignite. Class C components are mostly calcium oxide. Additionally, fly ash belonging to particular classes is determined by certain

parameters which they must meet. Chemical requirements for classes F, C and also for N – natural pozzolan (N)- are provided in Table 2 (ASTM C618-12).

Natural pozzolan is a ceramic building material that can be used as filler in a hydraulic mortar. Pozzolan main component is pure silica in the form of fine rounded grains. The important feature is the ability to bind the calcium [7].

Table 2 Chemical requirements concluded in ASTM C618-12 [46].

		Class		
		C	F	N
Silicon dioxide (SiO_2), Aluminum oxide (Al_2O_3), Iron oxide (Fe_2O_3),	min. %	50.0	70.0	70.0
Sulfur trioxide (SO_3),	max. %	5.0	5.0	4.0
Moisture content	max. %	3.0	3.0	3.0
Loss on ignition –LOI	max. %	6.0	6.0	10.0

In Figure 11 it is possible to observe the visual colour gradient of fly ash class F and class C in comparison with Portland cement, silica fume and ground-granulated blast-furnace slag (GGBF).

Figure 11 Comparison of fly ash class F and C, Portland cement, silica fume and GGBF slag [45].

Furthermore, fly ash can also be classified according to different standards, which are not universal, in terms of the loss of ignition (LOI), the fineness, the application of fly ash, the percentage of chemical components, etc.

3.2. Physical Properties

Characterization of physical properties of fly ash is based on description of fly ash grains, in particular their colour, shape, particle size distribution, density and bulk density.

Generally all fly ash are materials, displaying a colour range from light grey to black (depending on the content of carbon and unburnt organic parts, and magnetite grains), and brown (depending on the content of hematite and products of biomass combustion).

Fly ash is very heterogeneous in particle size distribution, which is greatly related with type of coal, degree of milling and type of the boiler, in which coal is combusted. At the same time, fly ash grains are highly diverse and distinguishable.

Grain size of fly ash formed in conventional boilers are in range of 0,01 to 350 μm, but occasionally larger grains may occur. The dominant grains show a spherical shape (mineral and amorphous grains) in the form of: filled pirosfers (constitute mainly of the finer ash fraction); blank cenospheres (constitute thicker ash fractions, with diameters greater than 100 μm); filled with smaller grains plerosfers. Filled grains are formed of melt minerals, and blank grains are formed of an alloy with a high share of gas phase. Usually grains can occur individually or as aggregated grains [8, 9].

According to some authors, who have developed a model for spherical grains, these grains are composed of a glass matrix, inside of which there are enclosed gas bubbles. In the subsurface layer of matrix, small crystals of mullite are embedded. The surface of the grain is covered by fine mineral crystals. Moreover, this surface is coated with a thin layer of electrostatically deposited graphite powder.

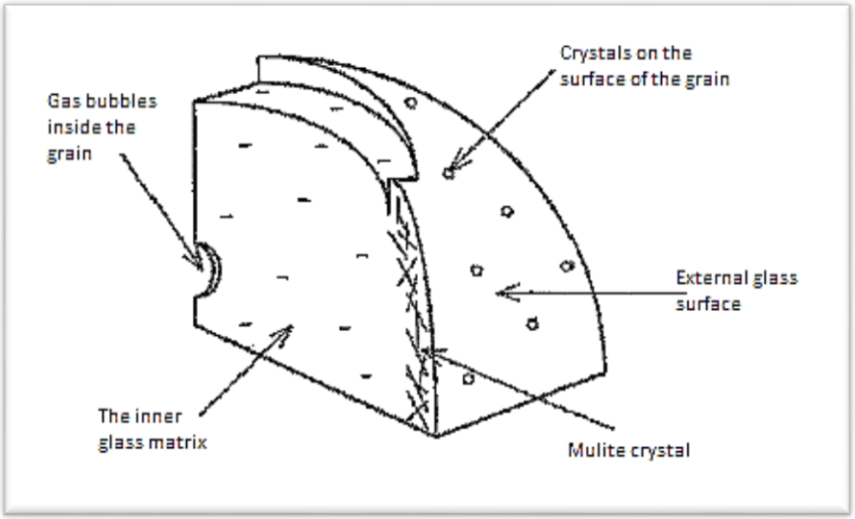

Figure 12 Model of the fly ash grain [48].

Apart from spherical grains, fly ash also contains irregular, highly porous with rounded or sharp-edged edges and rough or spongy surface grains. These grains can be classified according to their size and mineral composition. The largest grains are crumbs of unburnt carbon and soot and grains of quartz.

The finer fractions are formed of minerals, which structure was destroyed during thermal processes (decarbonation, dehydroxylation): however these grains were not melted. The finest fractions are mainly graphite dust. [8, 10, 11].

Unlike conventional fly ash, fly ashes from fluidized bed boilers have a slightly finer grain size distribution. In general, grain size does not exceed 100 μm. Spherical grains, characteristic of conventional ashes are practically absent in ash from fluidized bed boilers. Fluidized ash contains mostly grains with highly irregular shapes, elongated grains with sharp edges and isometric grains, lamellar and sharp-edged. These grains consist of dehydrated minerals forming the original gangue and have almost amorphous structure. Moreover, in this type of fly ash is frequent to find particles of larger dimensions, often with porous shapes close to spherical or oval. Mainly they are unburnt residues of coal and biomass. [12, 13, 14]

The density of fly ash is in the range between 1900 and 2800 kg/m^3. The range for conventional fly ash is round 2200 to 2500 kg/m^3. The density of fly ash from fluidized bed boiler is about 2500 to 2800 kg/m^3 and the bulk density of fly ash is between 400 to 1200 kg/m^3. Furthermore, another characteristic of fly ash is an extensive specific surface area, which is in range of 2500 to 6000 m^2/kg [8, 15, 16].

3.3. Chemical Composition

The chemical composition of fly ash changes over a wide range and depends on many factors like type of combusted fuel (coal, lignite, biomass) and type of installation (kind of boiler and technological conditions of combustion). Essentially, the chemical composition of fly ash is based on the chemical composition of the mineral matter of coal. However, there are differences in the chemical composition, because of the fact that fly ash is formed of only part of non-combustible components. The other part of mineral matter during the process forms slag or finest fractions of ashes which cannot be collected in the electrostatic precipitators. Additional differences in the chemical composition of fly ashes and mineral matter of coal are associated with the thermal transformation of minerals during combustion: dehydroxylation of loamy minerals, decarbonation of carbonates, sublimation of sulfur and alkalis, etc. Also, differences in the chemical composition are result of conditions of combustion process and type of the boiler. Higher temperature and a longer time of combustion results in more intensive sublimation of sulfur and alkali and thus their concentration in the fly ash is reduced. The boiler design affects the ratio of the quantity of fly ash to slag formation [15, 17, 18].

The main chemical components of fly ash are: SiO_2, Al_2O_3, FeO_3, CaO (95 - 99 %). Additionally, the secondary components are present in fly ash in the form of: MgO, Na_2O, K_2O, SO_3, P_2O_5, TiO_2 (0,5 – 3,5 %) and unburnt coal (losses on ignition). Content of coal in the ash is determined by: the particle size of combusted pulverized coal (the finer the coal is, then the lower content of unburnt coal is), temperature and time of combustion (the higher temperature and time of combustion is, then losses on ignition are lower) and construction of the hearth (fly ash obtained from fluidized bed boilers usually contain more carbon). Main and secondary components constitute in total 99,7 – 99,9 % of the overall mass of ash [43].

Table 3 Bulk chemical composition of coal fly ash dependent of the region [36].

Component	Range (mass%)				
	Europe[a]	US[b]	China[c]	India[d]	Australia[e]
SiO_2	28.5–59.7	37.8–58.5	35.6–57.2	50.2–59.7	48.8–66.0
Al_2O_3	12.5–35.6	19.1–28.6	18.8–55.0	14.0–32.4	17.0–27.8
Fe_2O_3	2.6–21.2	6.8–25.5	2.3–19.3	2.7–14.4	1.1–13.9
CaO	0.5–28.9	1.4–22.4	1.1–7.0	0.6–2.6	2.9–5.3
MgO	0.6–3.8	0.7–4.8	0.7–4.8	0.1–2.1	0.3–2.0
Na_2O	0.1–1.9	0.3–1.8	0.6–1.3	0.5–1.2	0.2–1.3
K_2O	0.4–4	0.9–2.6	0.8–0.9	0.8–4.7	1.1–2.9
P_2O_5	0.1–1.7	0.1–0.3	1.1–1.5	0.1–0.6	0.2–3.9
TiO_2	0.5–2.6	1.1–1.6	0.2–0.7	1.0–2.7	1.3–3.7
MnO	0.03–0.2	nd	nd	0.5–1.4	nd
SO_3	0.1–12.7	0.1–2.1	1.0–2.9	nd	0.1–0.6
LOI	0.8–32.8	0.2–11.0	nd	0.5–5.0	nd

Table 4 shows the major and trace elements in fly ash, according to various authors.

Table 4 Major and trace elements in coal fly ash [38].

Element	Coal fly ash						
	Page et al. (1979)	Adriano et al. (1980)	Jala and Goyal (2006)	Tripathi et al. (2009)	Pandey et al. (2009)	Riehl et al. (2010)	Lopareva-Pohu et al. (2011)
Major elements, g kg^{-1}							
Al	1–17.3	–[a]	312	–	4.8	108.5	0.47
Ca	1.1–222	5.4	34	0.029	–	86.4	1.84
Fe	10–290	16	68	0.0032	4	36.6	0.31
K	1.5–35	1.8	10.8	0.072	–	24.5	0.0021
Mg	0.4–76	1.2	1.4	0.017	–	11.5	0.019
P	0.4–8	0.5	10.8	0.0027	1.1	2.1	0.0024
S	1–15	20	0.02	0.058	–	2	0.013
Trace elements, mg kg^{-1}							
As	2.3–6300	–	6.2	BLD[b]	–	–	20.4
B	10–618	50	–	–	28.9	–	0.40
Cd	0.7–130	1.3	1.9	13.4	42.5	0.03	–
Co	7–520	7	58	21.1	–	26	17
Cr	10–1000	15	330	38.2	40.3	148	46
Cu	14–2800	19	0.002	65.8	58.4	57	38
Hg	0.02–1.0	0.18	–	BLD	–		0.40
Mn	58–3000	100	739	0.006	69.3	679	418
Mo	7–160	3.0	4.0	–	33.3	4.2	–
Ni	6.3–4300	15	13	44.2	204.8	88	48
Pb	3.1–5000	16	35	20.0	40.2	97	39
V	–	20	–	–	–	182	–
Se	0.2–134	3	3.6	–	–	–	–
Zn	10–3500	39	79	57.7	82.3	167	85

[a] Not measured.
[b] BLD – below the limit of detection.

The mercury content can reach 1 ppm , but is generally included in the range 0.01 - 1 ppm for bituminous coal. However fly ash also contains elements: Mn, B, Ba, Cu, Sr, Ni, Cr, Zn, Cd, Co, Mo, V, Se, Pb, As and other (0,1 – 0,3 %) and radioactive elements: K, Ra, Th. Trace elements constitute 0,1 to 0,3% of mass of waste but have a significant impact on the health of living organisms. The radioactive elements, although they are present in higher concentrations than in natural materials, generally do not exceed levels that prevent re-use of ash [9, 16, 19, 20, 57].

Individual grains of fly ash vary in their chemical composition. Generally, of the grains contain SiO_2, Al_2O_3, Fe_2O_3 and only some of the grains contain CaO, MgO, Na_2O, K_2O or SO_3. The diversity of the chemical composition of grains is large because of the fact that individual grains contain low amount of chemical compounds or are represented by the single compounds. Furthermore, some grains have magnetic properties. Quantity of magnetic fraction grows with increasing content of Fe_2O_3 in fly ash. Despite mentioned differences in the chemical composition of particular fly-ash, fly ash from the combustion of coal in the same boiler, have stable chemical composition [18, 21].

The pH of the fly ash is in the range from 4.5 to 12 depending on the sulfur content in coal as well as technology of combustion and flue gas desulfurization. Fly ash with acidic character have ratio of Ca to S lower than 2,5 while fly ash with upper ratio have alkaline character [17, 22].

3.4. Phase Composition

Fly ash in its phase composition include crystalline phase (mineral), vitreous phase (enamel silicon-aluminum) and amorphous phase (loamy).

The crystalline phase is present in fly ash from conventional boilers as well as fly ash from fluidized bed boiler, but in various types of boiler there are different composition of minerals. The composition of this phase consists of: primary minerals present in the coal (minerals with a high melting point and minerals which do not pass through combustion kernel because of the swirl in boiler); minerals which crystallized from the liquid phase; minerals which have arisen during the thermal treatment (thermal fusion products, e.g., dicalcium ferrite, and products of thermal dissociation such mullite, free lime); as well as minerals which arose as a result of polymorphic transformations of coal minerals as α-quartz, α-tridymite [13, 16, 18, 23].

The most common minerals in the fly ash are: quartz (β-SiO_2, α-SiO_2), mullite ($3Al_2O_3 \cdot 2SiO_2$ –not present in the fluidized ash), hematite (Fe_2O_3), magnetite (Fe_3O_4), magnesium oxide (MgO), calcite ($CaCO_3$), dolomite ($CaMg(CO_3)_2$), gypsum ($CaSO_4 \cdot 2H_2O$), anhydrite ($CaSO_4$), calcium oxide (CaO), proper spinel ($MgAl_2O_4$), spinel ($FeAl_2O_4$), dicalcium ferrite ($2CaO \cdot Fe_2O_3$), corundum (α-Al_2O_3), anatase or rutile (TiO_2), ettringite ($3CaO \cdot Al_2O_3 \cdot 3CaSO_4 \cdot 32H_2O$), opalit ($SiO_2$), and others [8, 24].

The vitreous phase occurs only in ashes from conventional boilers, being approx. 50 - 90% of total ash, the most common quantity is within the limits of 50 - 60%. The higher the combustion temperature, the increased glassy phase is formed [25].

The chemical composition of the glass resembles that of basalt. Fundamental units of structure of glass are tetrahedrons made of silicon oxides, aluminum oxides. Except those mentioned oxides, there are some alkaline metal oxides (modifying oxides, e.g. MgO, CaO, Na_2O, K_2O). They may constitute up to 50 % molar of silica. Fly ash can be divided into two varieties of glass : (i) Glass type I has low density, high ratio of content of SiO_2 to content of Al_2O_3, and low content of modifying oxides; (ii) Glass type II I characterized by high density, a low ratio of SiO_2 to Al_2O_3 content and high content of modifying oxides [24, 25].

The glassy phase is dispersed in the grains of fly ash. Grains composed of this phase are usually spherical, they often form aggregates with irregular shapes. The composition and structure of the vitreous phase is largely dependent on the particle size of fly ash. Type I of glass forms thicker, spherical grains of the ash, and glass type II forms finer, spherical and filled inside grains of fly ash. While content of glass is small in grains comprising high amounts of iron oxides [25, 26].

The amorphous phase is created mainly by dehydrated and dehydroxylated loamy minerals. In addition, it contains a small amount of amorphous carbon - carbon black. The amorphous phase is the predominant phase in the fly ash from fluidized bed boilers, whereas in conventional ashes this phase is present only trace amount [25].

4. Applications of fly ash

The application and economic utilization of by-products from coal combustion are determined by the type of coal used in a power plant or CHP plant, types of fuel combustion processes and technology of discharging by-products. The amount of by-products such as fly ash is higher in countries that depend on a large extent on coal utilization. Presently, the general trend shows that utilization of by-products is growing in many countries but there are still significant differences between developed countries, where the rate of utilization of by-products is increasing and the less developed ones where this use is not so stimulated. To illustrate the situation in the World, it is possible to use some figures: for example the rate of utilization of fly ash in USA increased from 8% in 1970, to 13% in 1980, to 25% in 1990 and 35% in 2002. In the case of UE, implementation of economic use of fly ash increased from 65% in 1997, to 88% in 2002, excluding recultivation works. This share increased, respectively, from 41% to 46%, while in other countries is for instance 84% for economic utilization of fly ash in Japan, 20% in Canada, 13% in India and only 5% in South Korea – figure 13 [15].

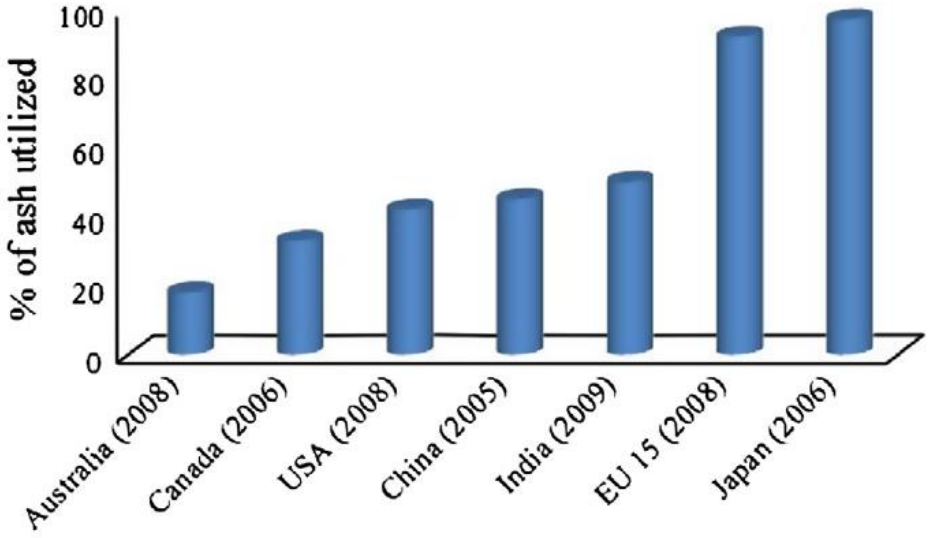

Figure 13 Utilization of fly ash in relation to total production in percentage [37].

In Poland the indicator of economic utilization of fly ash is particularly high and depending on the source, it increased from 82% to 96%, but only a small part is attributable to macro-levelling and recultivation works. Also in Poland there was a growth of fly ash utilization from 91,6% in 1998 to 96% in 2002 and 2003. The increased utilization of fly ash from coal combustion in Poland is due to significant use of this by-product as a substitute in construction industry [15].

4.1. Current applications

Fly ash applications have a significant impact in increasing industrial synergies. Presently, fly ashes derived from coal combustion are predominantly used in the construction industry as concrete additives.

Because of the pozzolanic properties of fly ash it can be used as a partial replacement for clinker (main component of Portland Cement) or other cementitious products in concrete.

Moreover, coal fly ash is also used in geotechnical applications which correspond to grouting, asphalt filling, pavement base course, structural fill, lightweight aggregates, soil amendment and other [15, 36].

4.2. Potential Applications

There are several potential applications to use fly ash. First of all fly ash can be used in direct applications without any pre-treatment. Secondly some components may be extracted or/and combined with chemical, thermal, mechanical methods and applied, which represents an indirect applications. And thirdly, fly ash can be divided into certain fractions and some of them can be used for specific purposes.

In this subsection several potential applications of coal fly ash such as adsorbent, soil improver in agriculture, catalysts, in ceramics and glass production, geopolymers, in high volume FA concrete production, mesoporous materials and zeolites will be described.

4.2.1. Adsorbents

It was found that coal fly ash can be used directly as an adsorbent in gaseous as well as in aqueous applications. The adsorbents important applications in pollution control. Coal fly ash adsorbents can be used to remove metal ions from waste waters with low costs. Metal ions that can be removed by coal fly ash are: Copper (Cu), Lead (Pb), Zink (Zn), Manganese (Mn), Cadmium (Cd), Chromium (Cr) and Nickel (Ni). However their usage is limited because of complex chemical composition of fly ash and required volumes fly ash for increased efficiency.

Coal fly ash have been investigated to be used in the same way as activated carbon for adsorption of phenol or typed of polychlorinated biphenyls. The investigation is suggests that, coal fly ash replace activated carbon because of lower adsorption properties; however, considering the low price of this by-products, fly ash can be alternative for removing organics from waste water.

Moreover, fly ash can be applied in flue gas desulphurization processes, where it is mixed with $Ca(OH)_2$. The principle is that when the ratio of CFA/$Ca(OH)_2$ increases, the reactivity during the process is also higher. This is due to a larger surface area that is obtained by mixing $Ca(OH)_2$ with coal fly ash [36].

4.2.2. Agriculture

Direct application of coal fly ash is possible in soil amelioration has important agronomic advantages. Fly ash as a soil additive can generally affects some soil physical properties, such soil texture, moisture retention capacity and chemical properties of soil such as pH, bulk composition and nutrient availability.

The main issue related to the use of coal fly ash is the pH level. Most of crops prefer a pH between the range of 6,5 – 7 for their optimum growth. Coal fly ash can be alkaline or acidic. Thus, when used, fly ash has to be matched perfectly to selected soil, because it cannot adversely modify the pH level of the

soil. Usually fly ash C is responsible for a raise in the pH of the soil. However when fly ash is added to soil with appropriate quantity and quality the soil can be modified favourably.

In addition, there are other advantages of using fly ash as a soil additive that include for example: increased soil aeration, reducing crust formation, reducing share of other soil amelioration like fertilizers and decreasing activity of metal in the soil. Besides advantages, there are also some disadvantages such as reduction of bioavailability of some nutrients caused by application of alkaline coal fly ash or surplus of salinity or toxicity. However, when coal fly ash is used in the appropriate manner it might show a positive effect on the soil as described in many publications [36, 37, 38].

4.2.3. Catalysts

Usually catalysts are made of materials which have limited reserves and/or are expensive to manufacture. Coal fly ash as a catalyst meets the requirements of being less expensive and available alternative material. Fly ash from coal fired power plant received a lot of attention in heterogeneous catalysis. Heterogeneous catalysis is superior in comparison to homogenous catalysis because it is easier to recover the catalysts after reaction. Moreover in heterogeneous catalysis, catalysts can be supported with other materials like metal oxides (Al_2O_3, SiO_2, TiO_2, MgO…). Coal fly ash mostly includes Al_2O_3 and SiO_2, therefore it can be used as support. Properties of fly ash such as thermal stability are indicated in the catalyst.

Nowadays, potential for coal fly ash as catalyst are highly investigated. There are plenty of applications as support material for nickel in the process of CO_2 methane reforming. Another one is for selective catalytic reduction of NO by ammonia with catalysts composed of coal fly ash with support materials Fe, Cu, Ni and V. The next application is in catalytic oxidation of volatile organic compounds (VOCs) where coal fly ash has been used as an active component. Other studies show that coal fly ash can be used to produce nano-crystalline solid acid catalyst by acid activation. Which may have application in production of acetylsalicylic acid (aspirin) and methyl salicylate (oil of wintergreen) [36, 51].

4.2.4. Geopolymers

Geopolymerisation is a technology where aluminosilicates are alkali-activated. The chemical reaction is between aluminosilicate oxides and alkali metal. Geopolymerisation takes place in strongly alkaline conditions, and provides amorphous or semicrystalline polymeric structures of Si-O-Al bonds. Products of geopolymerisation are so called geopolymers which are characterized by very good physical, chemical and mechanical properties. These properties include: low density, micro and nano-porosity, low shrinkage, high mechanical strength, thermal stability, hardness of the surface, resistance for fire and chemicals. Due to these properties, geopolymers are designed to be alternative materials for industrial applications (i.e. construction, transport etc.). However, the biggest attention is focused on the fact, that it can be use instead of ordinary Portland cement (OPC) as a binder in concrete applications.

In literature, there are plenty of analysis and tests about different coal fly ash used in geopolymers production. The results shows that alkali-activation of aluminosilicates strongly depends upon particle

size, morphology and chemical composition of raw materials used in a process for instance coal fly ash. It is proven that different coal fly ash, with different ratio of amorphous and crystalline components influenced final product. Geopolymers produced from fly ash with higher amount of crystalline fraction had lower mechanical strength in comparison to geopolymers produced with mostly amorphous fly ash. Also the chemical composition of fly ash can influence the geopolymers applications. For instance negative effects on the high temperature of geopolymers can arise if iron (Fe can appear in fly ash) – contents are increased [36, 40].

4.2.5. Ceramics and glass

Coal fly ash is composed of oxides such as SiO_2, Al_2O_3, CaO and Fe_2O_3. Fly ash composition makes it a suitable chemically compatible and low cost material to manufacture ceramics, glass-ceramics and glass materials. Manufacture of listed materials is the temperature which activates raw coal fly ash material with temperature changes, variations and co-reagents which influence on final form of glass or ceramic. The general schema of manufacturing ceramics, glass-ceramic and glass material is presented on Figure 14 where are shown general stages of the process without considering any additives [36].

Interestingly, physical and mechanical properties tests shows that glass and ceramics obtained from waste coal fly ash are well comparable with glass and ceramics produced with non-waste sources, regarding to literature values [36].

Manufacture of structural glass-ceramics is another appropriate application for coal fly ash due to its chemical composition. Especially, products received from class C coal fly ash, which contain minimum 50% of SiO_2, Al_2O_3 and Fe_2O_3 were characterized by high strength and acid resistance [36, 39].

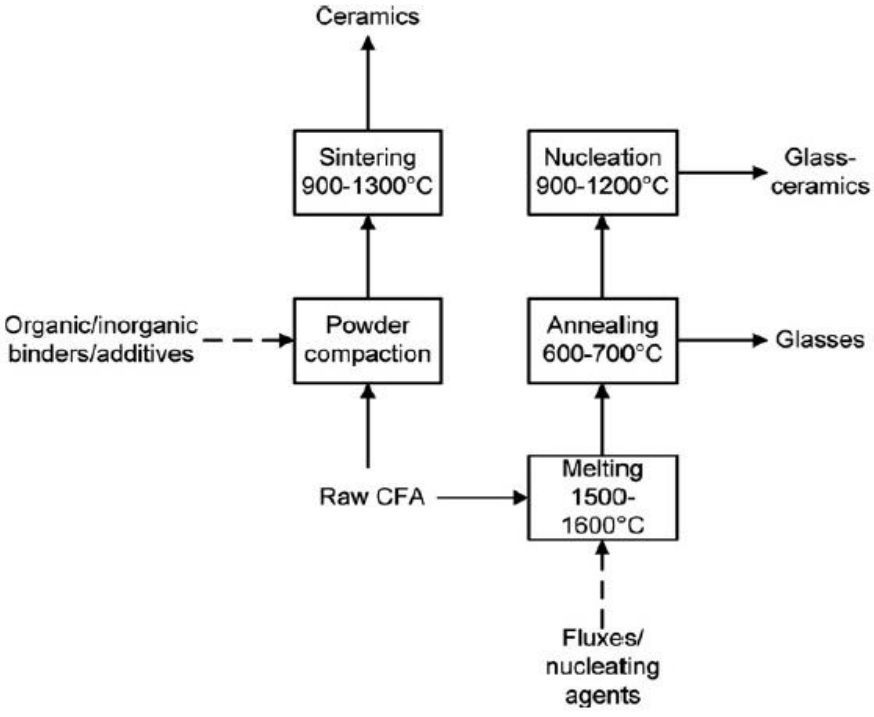

Figure 14 An overview of ceramics, glass and glass-ceramics production from coal fly ash (CFA) [36].

4.2.6. High volume fly ash concrete

Concrete is one of the most used materials in the world. There are several specifications which determine the limits of substitution. In concrete, addition of fly ash is limited to 15-20%. In fact it is proven that even bigger amount (25-30%) of substitution such as coal fly ash have beneficial influence on concrete. Substitution higher than 50% are referred as High Volume Fly Ash (HVFA) concrete.

High volume fly ash concrete consists of at least 50% of fly ash. Recently the interest about this type of concrete is greater, because of environmental and economic motives. HVFA concrete went through laboratory studies and the results are impressive. In comparison to conventional concrete, using high volume fly ash concrete has much more technical benefits such as: improved workability; higher early strengths and later strength; superior dimensional stability; electrical resistivity and resistance for chloride penetration; greater durability [36].

4.2.7. Mesoporous materials

Mesoporous materials are valuable from the point of view of their use in different separation and catalytic processes. Fly ash derived from coal combustion is a great source of silica for mesoporous silica production. Mesoporous silica is manufactured through methods similar to those used to prepare zeolites.

Via several different methods it is possible to obtain specified mesoporous materials such as MCM-41 or Al-MCM-41 (which comprises aluminium), SBA-16 and others from coal fly ash [36].

4.2.8. Zeolites

Zeolites due to its structure are very suitable materials in processes of adsorption. In zeolites manufacture, a source of Si and Al ions is required. Zeolitisation also needs an alkaline environment and usually high temperature. The process depending on the reactants and process conditions may take from days to even months. Fly ash due to its high content of aluminium and silica ions is a good source for zeolites synthesis.

There are a lot of variations in zeolite manufacture methods and yields, which can result in different zeolite types: it is possible to obtain 13 different types of zeolites from the same fly ash. Generally temperatures of zeolites synthesis by one stage hydrothermal method are between range 125 – 200^{o}C but there are also methods where temperatures are above 500^{o}C, like in the pre-fusion method [36]. To simplify the approaches of various methods, they are presented in figure 15.

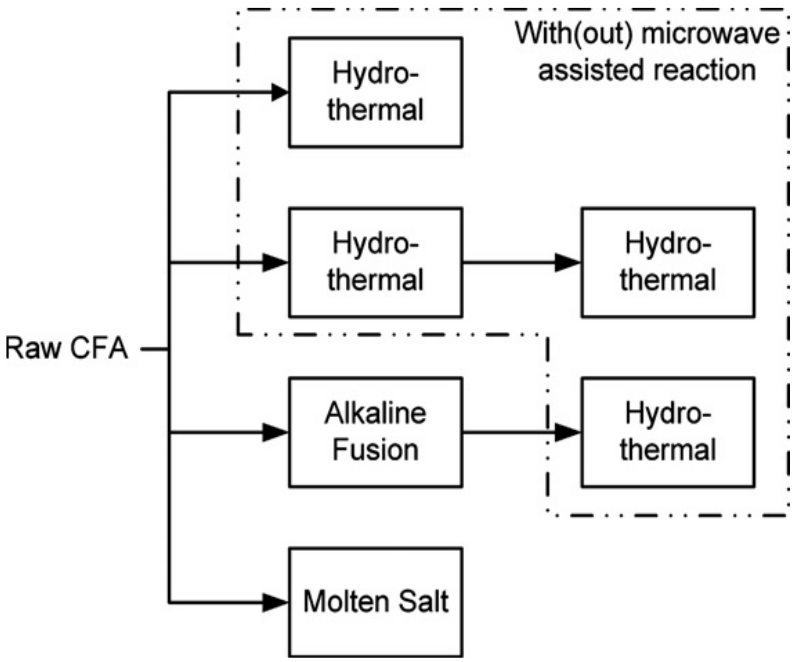

Figure 15 Various experimental approaches of zeolites synthesis from coal fly ash [36].

Figure 15 shows that besides one stage hydrothermal treatment of raw coal fly ash there is also method with two stages of hydrothermal processes. Moreover, raw fly ash can be treated by hydrothermal process with prior alkaline fusion or by molten salt method. The last method is rather unusual and, interestingly water is not used at all in this process. Moreover not every method use microwave radiation which aims to reduce the conversion time of zeolite synthesis from fly ash [36, 46].

4.3. Applications for separated fractions

Coal fly ash is usually composed of plenty of components, which have raised a lot of interest these days and can be significantly useful after separation. There are many publications in which different techniques of separation components have been investigated.

Generally, fly ash from coal combustion can be divided into various fractions as follows: concentration of ceramic cenosphere (CCC), concentration of water soluble salt (WSC), magnetic concentrate (MC), char concentrate (CC), heavy concentrate (HC), and improved fly ash residue (IFA). Sequential fly ash schematic separation is presented in figure 16.

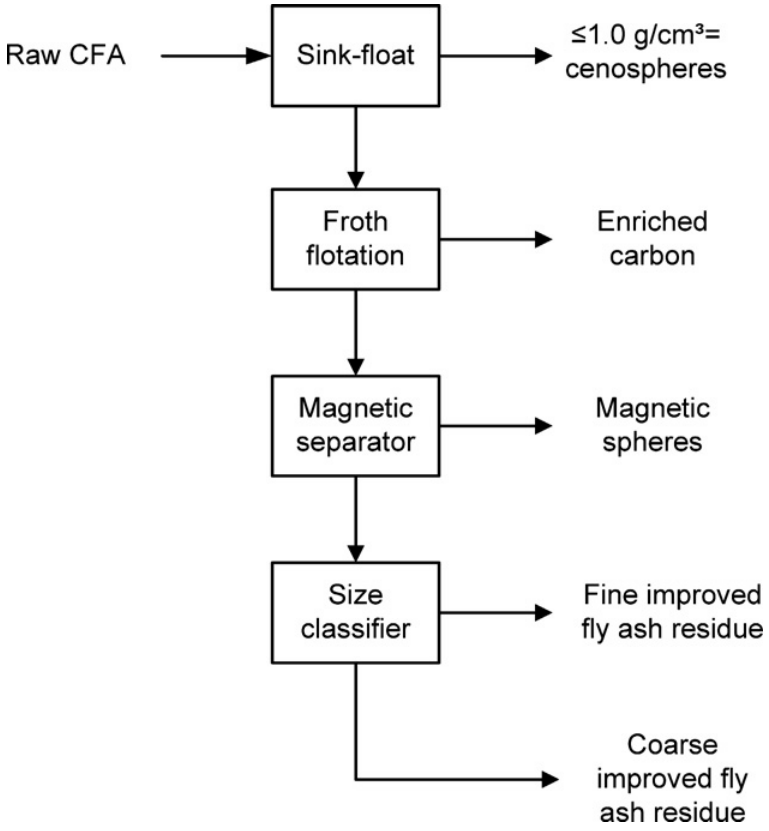

Figure 16 Possibilities of coal fly ash separation [36].

In this subsection three most advanced and promising fractions of fly ash: (i) unburnt carbon, (ii) cenospheres, (iii) magnetic spheres, with their removal techniques will be described.

4.3.1. Carbon

Coal fly ash always contains some amount of unburnt carbon which can be liberated and then can be applied. The most often method used for carbon recovery from fly ash is froth flotation. This separating method is based on the ability of air bubbles to adhere to selected mineral surface. Particles which are connected to the air bubbles rise through the slurry, while other residues sink to the bottom of the vessel. Carbon is hydrophobic, thus, based on knowledge connected to this issue flotation cell was invented and commercialised in the US. The recovery grade of carbon in mechanical froth flotation cell or flotation column amounts is up to 70%. There are also other methods as oil agglomeration or triboelectrostatic separators but not so frequently used.

Recovered carbon from fly ash may have plenty of potential applications. First application could be to use carbon as coke in the metallurgical industry. However there are some restrictions which define the phosphorous content.

Also enriched carbon from coal fly ash can be used in preparation of activated carbon. Activated carbon manufactured from fly ash may be applied for sulphur dioxide (SO_2) or NO_x removal from flue gases or treatment of liquid wastes. Another application of unburnt carbon is in manufacture of graphite. Generally in all applications unburnt carbon is a cheaper replacement.

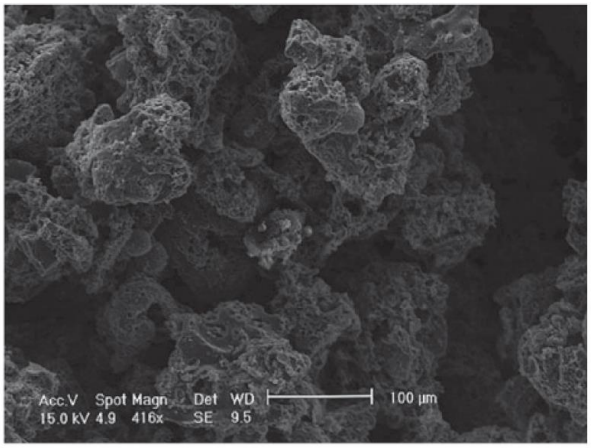

Figure 17 SEM image for unburnt carbon in fly ash [36].

4.3.2. Cenospheres

Coal fly ash is rich in cenospheres which are one of the most important components of this fraction. These hollow spherical particles are characterized by compositions similar to fly ash but tend to have bigger particle diameter.

The method of extraction is based on the difference of density. Cenospheres have lower density relatively to water. The principle of the operation is that when fly ash is mixed with water for example in a lagoon, the cenopheres can be collected from water surface. Unfortunately, this method requires large areas and is time intensive. The possible alternative method is to use triboelectric separation systems, where as defined specific gravity of cenospheres is less than 2. However any subsequent method is not as effective as wet separation of cenospheres from coal fly ash.

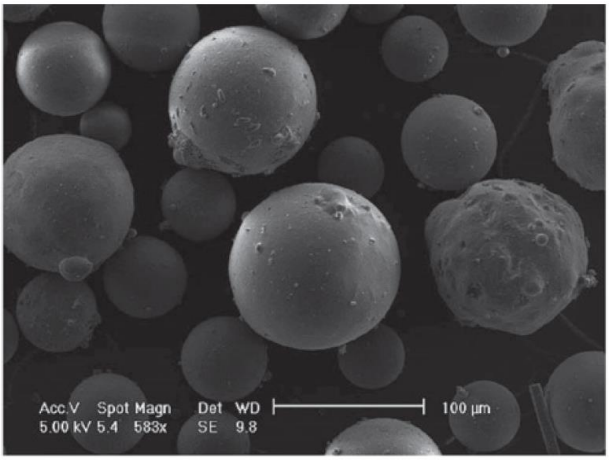

Figure 18 SEM image for cenospheres in fly ash [36].

Cenospheres deserved great attention because of their unique properties. Their sphericity and low density make them suitable for plenty of applications. Cenospheres can be applicable in new photocatalysts where float features are required to easily recover particles from water after reaction. Also cenospheres in combination with magnesia can be useful in water purification, especially to remove

surplus of fluoride from drinking water. Cenosphere properties make them suitable for application in lightweight materials (in electromagnetic fields) or light weight composite materials for example in concrete, polymers and metal alloys. Economically the use of cenospheres from coal fly ash is reasonable because it is very interesting fraction which can have much more potential applications these mentioned above [36].

4.3.3. Magnetic spheres

Magnetic spheres in coal fly ash can also create an opportunity for added value. This fraction is highly dependent on the coal source and operating conditions in the boiler. The magnetic material may constitute from 0,5% up to 18%.

The removal of magnetic spheres from fly ash relies on the fact that different materials have their own moment of magnetic moments which react during forces in presence of magnetic field gradients. That means the external application of magnetic field can lift out materials with the same magnetic properties.

Figure 19 SEM image for magnetic sphere in fly ash [36].

Feasible application of magnetic fraction from fly ash is in coal cleaning circuits where magnetite works as a dense medium separation. Furthermore magnetite could be used as a filler material in polymers, thermoplastics or rubbers [36].

Taking into account the discussions above, it is clear that fly ash, despite of its status, as waste or by-product can be successfully used in many areas. The list of possible fly ash applications is extensive, but the key issue to use fly ash is to have detailed knowledge on its properties. Therefore it is crucial to perform studies for full characterisation of fly ash fractions. To meet these requirements fly ash samples of different origins must be studied in detail. Thus, in this work a specific fraction supplied by EDF Polska S.A. R&D Center was studied and its relevant properties detailed by using a powerful combination of microscopic and analytical methodologies. Hopefully, this knowledge can guide industry in the understanding of the byproduct properties and in finding proper application to disclose this materials.

5. Methodology

5.1. Origin of the fly ash samples

Samples used in the experimental work reported in this dissertation where provided by EDF Polska S.A. R&D Center. This material is fly ash from hard coal fired power plant from a specific unit. The boiler producing this material is a boiler- type OP-650 and the turbine is condensing-type. The electrical capacity of this unit is 225 MW, while fuel capacity is 589 MWt. Additional technical data about this unit is presented in table 5.

Table 5 Technical data referring to the unit from which fly ash samples where obtained.

Technical data	
Fuel capacity	589 MWt
Output capacity	530 MWt
Gross electric capacity	225 MWe
Own consumption	18.3 MWe
Steam temperature (live/reheated)	540 ^{o}C / 540 ^{o}C
Steam pressure (live/reheated)	13.5 MPa / 2.5 MPa
Net electric capacity	206.9 MWe

The fly ash samples were delivered at 06.06.2014.

5.2. Separation of the fractions

The first step consisted on the separation of fly ash into various fractions using a series of sieves with different mesh sizes. With such equipment it was possible to obtain fractions with different granulometry and characteristic particle size. This step was crucial since it is necessary the characterization of the particles according to various characteristic diameters. To separate the different fractions of fly ash the following sieves (characteristic mesh size) were used: 320 μm with square mesh shape and 200 μm, 100 μm, 63 μm with round mesh shape. The sieving was done manually, except for the smallest fraction under 63 μm, which was done mechanically.

Thus, the fractions where divided in the following ranges:

1) Fly ash particles above 320 μm;
2) Fly ash particles between 320 – 200 μm;
3) Fly ash particles between 200 – 100 μm;
4) Fly ash particles between 100 – 63 μm,
5) Fly ash particles under 63 μm.

During screening of the fly ash samples, each fraction was weighed and the weight percentage of each fraction was calculated with regard to the total ash mass. All calculations, including arithmetic averages and standard deviations are presented in table 6.

Table 6 Percentage of each fraction referring to the total mass of fly ash, arithmetic average and standard deviation.

Sample number / **Fraction**	**1** **[%]**	**2** **[%]**	**3** **[%]**	**4** **[%]**	**Arithmetic Average**	**Standard deviation**
Above 320 μm	0.18	0.22	0.2	0.2	0.200	0.016
320 - 200 μm	1.56	1.74	1.64	1.85	1.698	0.126
200 – 100 μm	16.8	17.11	16.45	15.5	16.465	0.698
100 – 63 μm	20.71	20.73	20.93	19.67	20.510	0.569
Under 63 μm	60.75	60.2	60.78	62.78	61.128	1.133

It is worth to notice that the obtained fractions, despite the differences in particle sizes, also differ visually in colour. The visual colour changes are presented in figure 19. The following trends can be outlined: the fraction of largest diameter contains more black particles; while the smallest fractions are almost entirely grey. It can be stated that according to the particle size, from the smallest to the largest, the colour gradually becomes more intense and darkens – Figure 20. In addition, by comparing the separated fractions with the initial (non-sieved) samples of ash, the dominant colour allows noticing which fractions are dominant.

1) Above 320 µm	4) 100-63 µm
	
2) 320-200 µm	**5) Under 63 µm**
	
3) 200-100 µm	**6) Total fly ash**
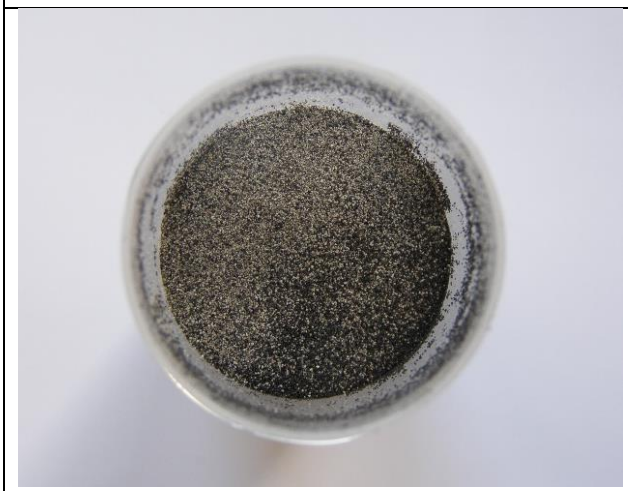	

Figure 20 Photographs of different fractions (1, 2, 3, 4, 5) and total fly ash (6) made by digital camera.

5.3. Size range measurement

Measurements to detail the size of the fly ash particles were carried out using a Malvern Mastersizer 2000 equipment developed by the Malvern company.

Mastersizer 2000 is an instrument, which is based on laser light scattering. During the measurement, particles are passed through a focused laser beam as it is shown on figure 21. Then these particles scatter the light at an angle which is inversely proportional to the particle size. The angular intensity of the light is measured by photosensitive detectors. The fundamental principle of calculating the particle size is based on the intensity of scattering and corresponding angles. The Mastersizer 2000 software applies the Mie scattering model. Mastersizer 2000 can be used to measure both dry and wet samples, which makes this instrument a very flexible one. In addition, the system allows the measurement of particles sizes ranging between 0.02 – 2000 μm, with an accuracy better than 99% [52, 53].

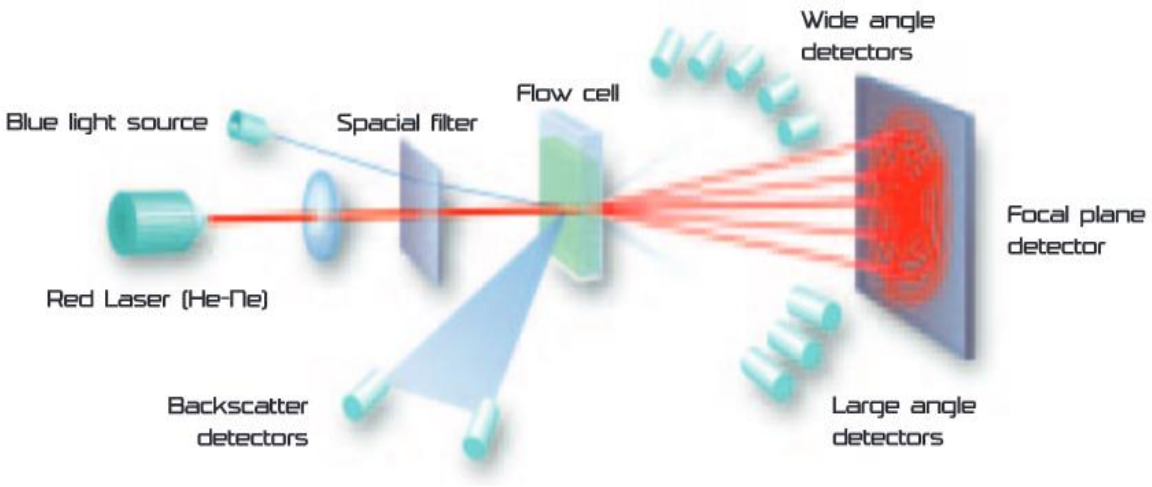

Figure 21 Schema of principle of operation in the instrument Mastersizer 2000 [53].

Capabilities of the above-mentioned instrument were very useful since the precise measurement of fly ash particle size is of great importance for the interpretation of all results.

Samples taken from the original fly ash batch were subjected to the test. Ten measurements were performed for the different samples. Each sample was analyzed in terms of the content of particle size in the specific ranges. Table 7 presents all particle size ranges, average diameter of a range and values corresponding to arithmetical average of quantity [in %] of particles detected in given range, for all ten samples of fly ash.

Table 7 Values obtained from Mastersizer 2000.

No	Diameter range [µm]			Dav [µm]	AV [%]
1	0,01	-	0,011	0,0105	0,000
2	0,011	-	0,013	0,012	0,000
3	0,013	-	0,015	0,014	0,000
4	0,015	-	0,017	0,016	0,000
5	0,017	-	0,02	0,0185	0,000
6	0,02	-	0,023	0,0215	0,000
7	0,023	-	0,026	0,0245	0,000
8	0,026	-	0,03	0,028	0,000
9	0,03	-	0,035	0,0325	0,000
10	0,035	-	0,04	0,0375	0,000
11	0,04	-	0,046	0,043	0,000
12	0,046	-	0,052	0,049	0,000
13	0,052	-	0,06	0,056	0,000
14	0,06	-	0,069	0,0645	0,000
15	0,069	-	0,079	0,074	0,000
16	0,079	-	0,091	0,085	0,000
17	0,091	-	0,105	0,098	0,000
18	0,105	-	0,12	0,1125	0,000
19	0,12	-	0,138	0,129	0,000
20	0,138	-	0,158	0,148	0,000
21	0,158	-	0,182	0,17	0,000
22	0,182	-	0,209	0,1955	0,000
23	0,209	-	0,24	0,2245	0,000
24	0,24	-	0,275	0,2575	0,000
25	0,275	-	0,316	0,2955	0,000
26	0,316	-	0,363	0,3395	0,000
27	0,363	-	0,417	0,39	0,000
28	0,417	-	0,479	0,448	0,000
29	0,479	-	0,55	0,5145	0,000
30	0,55	-	0,631	0,5905	0,000
31	0,631	-	0,724	0,6775	0,000
32	0,724	-	0,832	0,778	0,000
33	0,832	-	0,955	0,8935	0,000
34	0,955	-	1,096	1,0255	0,000
35	1,096	-	1,259	1,1775	0,000
36	1,259	-	1,445	1,352	0,000
37	1,445	-	1,66	1,5525	0,000
38	1,66	-	1,905	1,7825	0,000
39	1,905	-	2,188	2,0465	0,000
40	2,188	-	2,512	2,35	0,292
41	2,512	-	2,884	2,698	0,579
42	2,884	-	3,311	3,0975	0,741
43	3,311	-	3,802	3,5565	0,932
44	3,802	-	4,365	4,0835	1,131
45	4,365	-	5,012	4,6885	1,350
46	5,012	-	5,754	5,383	1,573
47	5,754	-	6,607	6,1805	1,785
48	6,607	-	7,586	7,0965	1,979
49	7,586	-	8,71	8,148	2,151
50	8,71	-	10	9,355	2,299
51	10	-	11,482	10,741	2,439
52	11,482	-	13,183	12,3325	2,568
53	13,183	-	15,136	14,1595	2,691
54	15,136	-	17,378	16,257	2,791
55	17,378	-	19,953	18,6655	2,858
56	19,953	-	22,909	21,431	2,884
57	22,909	-	26,303	24,606	2,899
58	26,303	-	30,2	28,2515	2,960
59	30,2	-	34,674	32,437	3,101
60	34,674	-	39,811	37,2425	3,293
61	39,811	-	45,709	42,76	3,459
62	45,709	-	52,481	49,095	3,546
63	52,481	-	60,256	56,3685	3,608
64	60,256	-	69,183	64,7195	3,815
65	69,183	-	79,433	74,308	4,262
66	79,433	-	91,201	85,317	4,788
67	91,201	-	104,713	97,957	5,070
68	104,713	-	120,226	112,47	4,938
69	120,226	-	138,038	129,132	4,520
70	138,038	-	158,489	148,264	4,103
71	158,489	-	181,97	170,23	3,833
72	181,97	-	208,93	195,45	3,510
73	208,93	-	239,883	224,407	2,913
74	239,883	-	275,423	257,653	2,057
75	275,423	-	316,228	295,826	1,220
76	316,228	-	363,078	339,653	0,412
77	363,078	-	416,869	389,974	0,136
78	416,869	-	478,63	447,75	0,152
79	478,63	-	549,541	514,086	0,158
80	549,541	-	630,957	590,249	0,149
81	630,957	-	724,436	677,697	0,058
82	724,436	-	831,764	778,1	0,000
83	831,764	-	954,993	893,379	0,000
84	954,993	-	1096,48	1025,74	0,000

Results obtained from Malvern Mastersizer 2000 apparatus, were gathered and analysed. All ten surveys were presented in the form of a graph. Figure 22 shows the distribution of the 10 samples of coal fly ash analysed.

As it is noticeable on the graph, there are no significant discrepancies, which mean that all fly ash samples are nearly uniform. There is only one range, for which some discrepancy appears. This is located at the larger diameter size of the graph. This means that the segment with largest particle size, above 340 µm, is shows the largest ranges of differences which vary from 0,8% to almost 0% occurrence of the particles in the samples. This result is intelligible because in fly ash the largest fractions contain mostly unburnt carbon. Still, the range of divergences is not significant in relation to the total of fly ash.

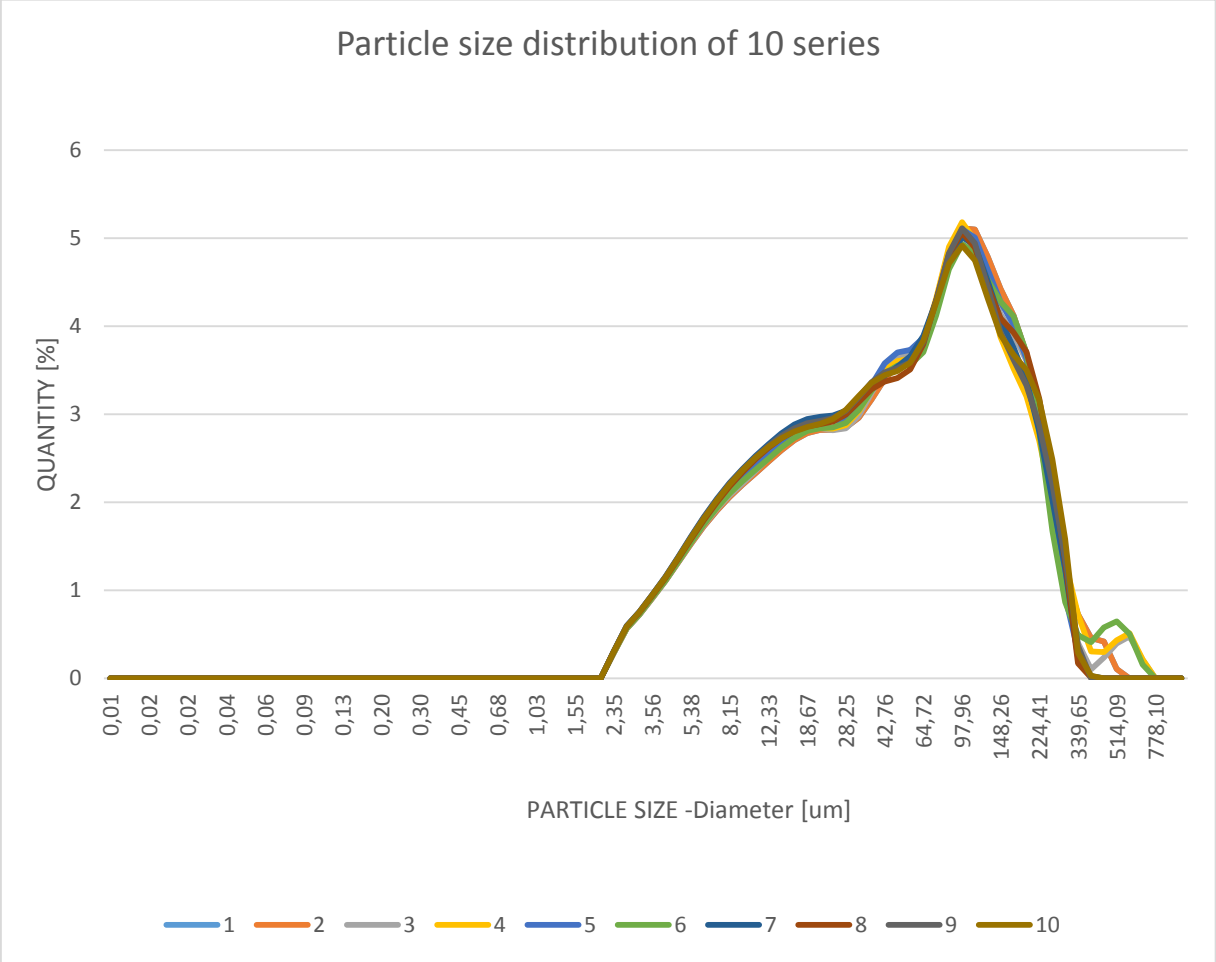

Figure 22 Quantitative profile of fly ash particles dependent of diameter size of 10 surveys.

All 10 measurements were averaged by the corresponding arithmetic average and another graph could be obtained (Figure 23). This graph shows the mean particle size distribution of the fly ash. Generally, fly ash particles start to appear around 2 µm and vanish around 700 µm. There is a growing trend from 2 µm up to 100 µm, where the highest peak of the function is observed. Afterwards there is a decreasing trend to around 320 µm and then a slight growth transformed into a permanent position until the end of the plot.

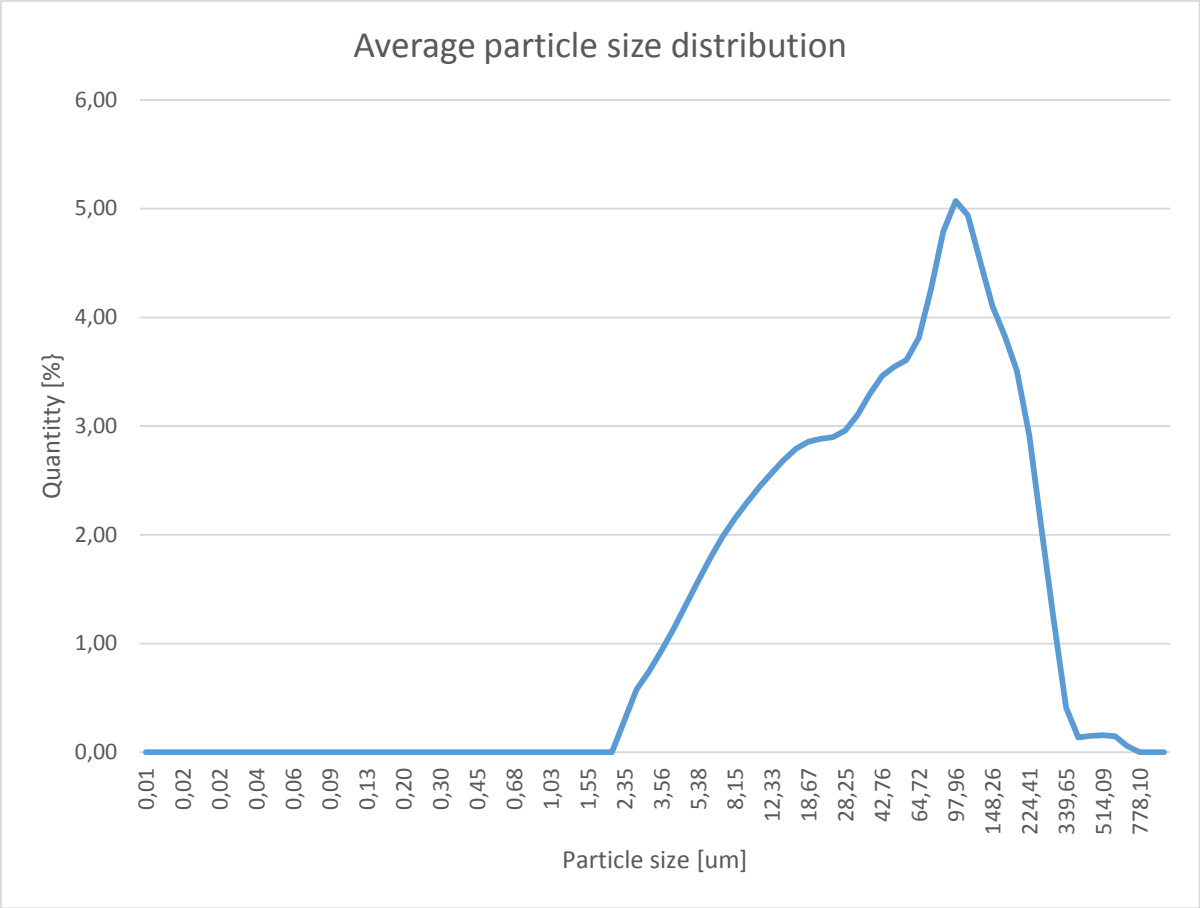

Figure 23 Average quantitative profile of fly ash particles dependent of diameter size

Consequently, the most numerous range of fly ash particles is when their size is around 100 μm. The second in terms of quantity is part between 100 μm up to 320 μm. Less numerous but appearing in larger area is part between 2 μm and 100 μm. Moreover, after a careful analysis it can be stated that this part, between 2 μm and 100 μm, embrace the largest percentage of the tested fly ash. On the other hand, almost quantitatively negligible is part above 320 μm.

5.4. SEM and EDX

The scanning electron microscope (SEM) is a tool commonly used in materials characterization. The technique makes use of a focused beam of high energy electrons to produce a diversity of signals at the surface of the sample. The signals provide information about morphology (texture), microstructure and chemical composition of the specimens. The SEM analysis provides data from a selected area of sample's surface and with this data it is possible to generate 2-dimensional images, from which morphological variations changes can be observed. The SEM technique (depending on the system), can work in the magnification range from 20X to 30,000X and can provide the spatial resolution between 50 and 100 nm.

The SEM is also able to perform analyses of selected points located on the area under analysis. This technique can be coupled with a detector, and it is possible to determine the elemental composition by EDS.

In the scanning electron microscope (Figure 24), the signals are originated from the interaction between high energy electrons and matter. This interactions results in various phenomena that include release of electrons such as the secondary electrons (which produce SEM image) and/or backscattered electrons (BSE). Secondary electrons are very valuable assessing the morphology of the sample, while backscattered electrons are especially useful for illustrating contrasts in composition in multiphase samples [55, 56].

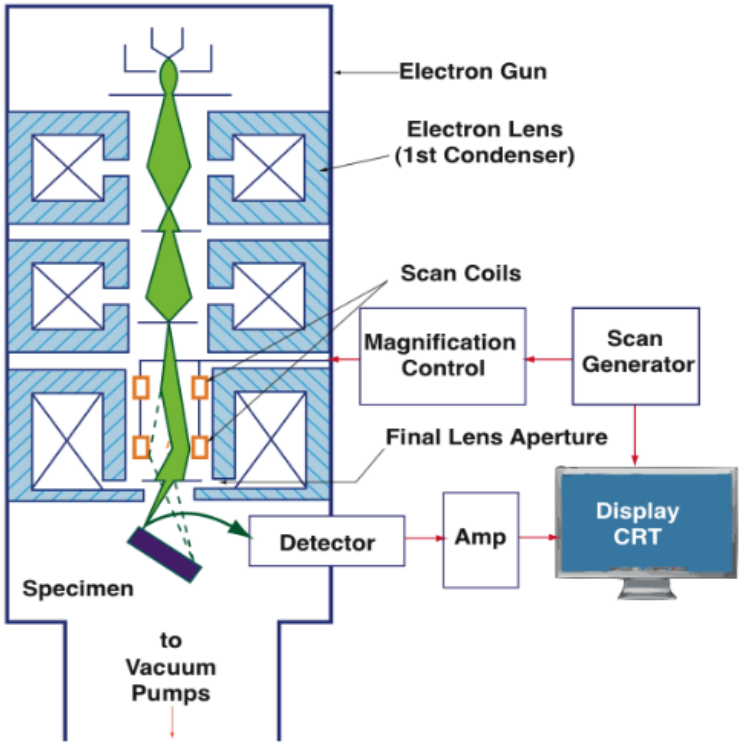

Figure 24 Scanning electron microscope scheme [54].

Other signals emitted from the surface are related to characteristics X-rays, which result from energy dispersive X-rays analysis (EDX) and are produced by inelastic collisions of the incident electrons with other electrons in discrete orbitals (shells) of atoms in the sample. This analysis technique is typically coupled with scanning electron microscopes. EDX allows to determine the chemical composition and almost all element can be detected [55].

In this work, SEM and EDX analysis were carried out for the specified fractions at the microscopy laboratory of Instituto Superior Tecnico (IST) in Lisbon, using Hitachi SEM, model S2400, with a tungsten filament and image acquisition using the Quantax Esprit software, equipped with the detector SDD from Bruker. The measurements were performed using an electron beam with energy of 25 kV. Moreover, samples were covered with gold alloy to obtain conductivity, thus, gold signal can be observed in the EDX analysis. SEM and EDX analysis were performed for each fraction separately. Therefore, images and graphs were obtained for five different fractions.

The experiments of non-separated fly ash samples were performed in a microscopy laboratory at University of Science and Technology (AGH) in Kraków. The images of the powders were recorded using a FEI Nova NanoSEM 200 microscope equipped with low vacuum detector. The presentation of the results, starts with the ones obtained for the non-separated fly ash and then the results obtained in separated fractions, from the smallest up to the greatest, are presented.

5.4.1. Non-separated fly ash characterization

Total fly ash characterization is essential characterize the original by-product as a whole. Therefore, Figures 25 and 26 depict the SEM images of the “as received” fly ash samples. Particles presented on the figures are highly diversified concerning sizes and shapes. It is possible to find very large particles as well as so small ones that are barely visible. Moreover, the shape of the particles vary from very regular spherical shapes to completely irregular, weird shaped particles. In order to properly characterize fly ash, six different particles from each figure were selected and analyzed in terms of chemical composition.

Thus, for each particle there is a table depicting the elemental composition (tables 8 – 13) for particles from figure 25 and tables 14 - 19 for particles from figure 26. Generally, the elemental composition of all particles consisted of the same elements but in different concentrations. The major elements detected are as follows: C, O, Na, Mg, Al, Si, K, Ca, Ba, Fe. There are some trace amounts of Pb and Cu.

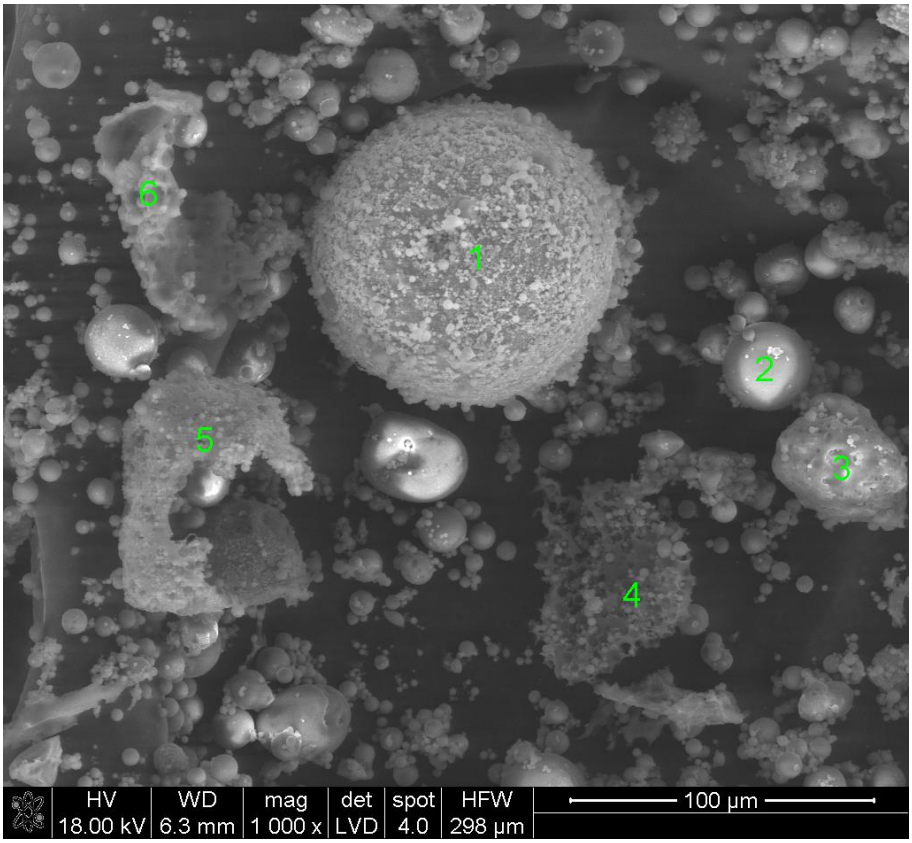

Figure 25 SEM image for fly ash sample, and 1000 magnification.

Table 8 The quantitative elemental composition of particle 1 from Figure 25.

1	C	O	Na	Mg	Al	Si	Pb	K	Ca	Ba	Fe	Cu
% wt.	11.22	32.16	0	4.73	6.61	4.79	1.14	0.72	0.51	1.77	35.59	0.76
% at.	21.97	47.26	0	4.57	5.76	4.01	0.13	0.43	0.3	0.3	14.98	0.28

Table 9 The quantitative elemental composition of particle 2 from Figure 25.

2	C	O	Na	Mg	Al	Si	Pb	K	Ca	Ba	Fe	Cu
% wt.	17.06	37.71	0.75	2.82	11.7	18.87	0.21	0.76	5.99	1.75	2.19	0.2
% at.	27.02	44.84	0.62	2.21	8.25	12.78	0.02	0.37	2.84	0.24	0.74	0.06

Table 10 The quantitative elemental composition of particle 3 from Figure 25.

3	C	O	Na	Mg	Al	Si	Pb	K	Ca	Ba	Fe	Cu
% wt.	15.48	41.09	0.76	0.99	14.72	19.56	0.17	2.25	1.92	1.22	1.85	0
% at.	24.22	48.27	0.62	0.76	10.25	13.09	0.02	1.08	0.9	0.17	0.62	0

Table 11 The quantitative elemental composition of particle 4 from Figure 25.

4	C	O	Na	Mg	Al	Si	Pb	K	Ca	Ba	Fe	Cu
% wt.	68.52	14.03	0.52	0.36	4.81	6.37	0.94	1.08	0.46	1.23	1.69	0
% at.	80.27	12.34	0.32	0.21	2.51	3.19	0.06	0.39	0.16	0.13	0.42	0

Table 12 The quantitative elemental composition of particle 5 from Figure 25.

5	C	O	Na	Mg	Al	Si	Pb	K	Ca	Ba	Fe	Cu
% wt.	53.51	24.61	0.55	0.57	6.61	8.16	0.77	1.42	1.04	0.9	1.87	0
% at.	66.68	23.02	0.36	0.35	3.67	4.35	0.06	0.54	0.39	0.1	0.5	0

Table 13 The quantitative elemental composition of particle 6 from Figure 25.

6	C	O	Na	Mg	Al	Si	Pb	K	Ca	Ba	Fe	Cu
% wt.	76.74	9.66	0.31	0.46	3.78	4.77	1.05	0.86	0.51	0.86	1	0
% at.	86.35	8.16	0.18	0.25	1.9	2.29	0.07	0.3	0.17	0.08	0.24	0

Consequently, particles not only differ morphologically, but they also differ in terms of composition. For example in some particles copper was detected and in some others sodium was absent. Especially, the composition of particle 1 (table 8) differs from the others, due to lack of sodium and very high content 35.59 % wt. of iron. For comparison, the remaining particles contain approximately 1-2 % wt. of iron. Particle 1 represents a magnetic sphere. Particles 2 and 3, apart from similar shapes, also present almost similar composition. They have a higher content of silicon and aluminum, as well as carbon and oxygen. Their composition indicate that they are cenospheres. On the other hand, particles 4, 5 ,6 show similar composition. Their content of carbon is higher than in other particles and, in addition, their shapes are totally irregular. It can be considered that these are particles of unburnt carbon.

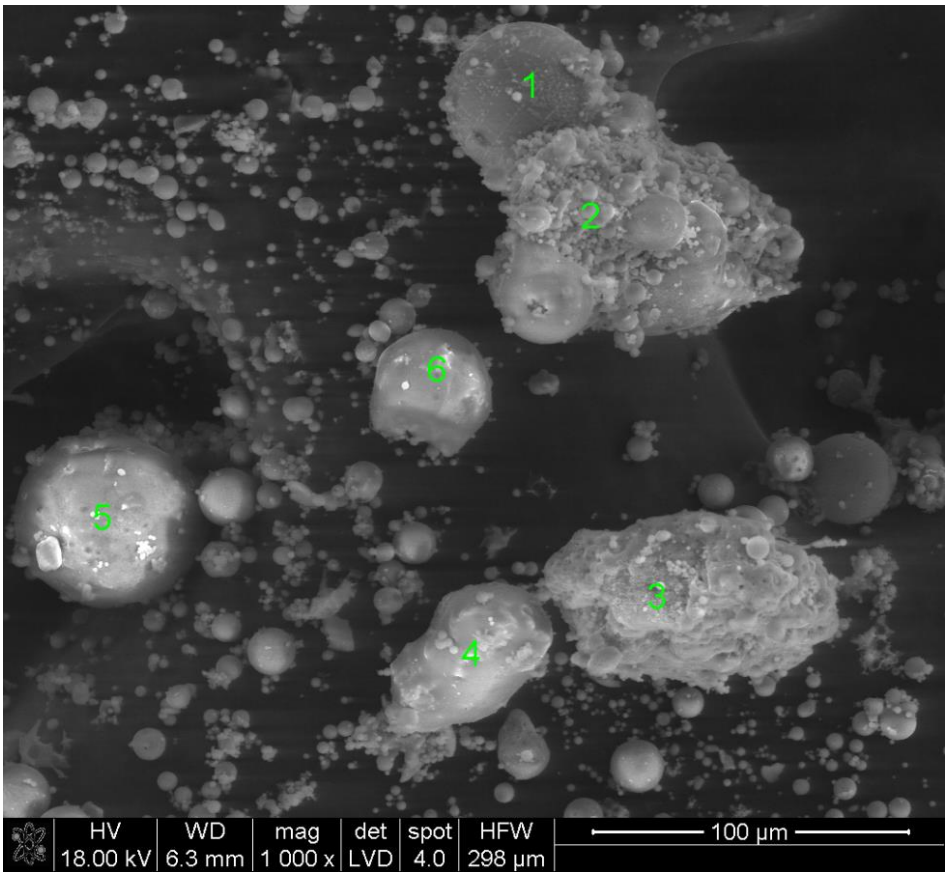

Figure 26 SEM image for fly ash sample, 1000x magnification.

Table 14 The quantitative elemental composition of particle 1 from Figure 26.

1	C	O	Na	Mg	Al	Si	Pb	K	Ca	Ba	Fe	Cu
% wt.	20.26	37.33	0.29	2.6	6.13	10.99	0.28	0.63	2.94	1.06	17.14	0.35
% at.	32.63	45.14	0.24	2.07	4.39	7.57	0.03	0.31	1.42	0.15	5.94	0.11

Table 15 The quantitative elemental composition of particle 2 from Figure 26.

2	C	O	Na	Mg	Al	Si	Pb	K	Ca	Ba	Fe	Cu
% wt.	19.34	42.72	1.34	0.9	11.76	18.13	0.33	2.22	0.37	0.75	2.12	0
% at.	28.92	47.95	1.05	0.66	7.83	11.59	0.03	1.02	0.17	0.1	0.68	0

Table 16 The quantitative elemental composition of particle 3 from Figure 26.

3	C	O	Na	Mg	Al	Si	Pb	K	Ca	Ba	Fe	Cu
% wt.	18.24	37.13	1.14	1.05	11.46	16.77	0.68	2.39	0.84	1.79	8.51	0
% at.	29.17	44.59	0.95	0.83	8.16	11.47	0.06	1.17	0.4	0.25	2.93	0

Table 17 The quantitative elemental composition of particle 4 from Figure 26.

4	C	O	Na	Mg	Al	Si	Pb	K	Ca	Ba	Fe	Cu
% wt.	52.76	25.95	0.41	0.5	3.74	11.49	0.39	1.19	0.7	0.92	1.95	0
% at.	65.64	24.24	0.27	0.31	2.07	6.11	0.03	0.45	0.26	0.1	0.52	0

Table 18 The quantitative elemental composition of particle 5 from Figure 26.

5	C	O	Na	Mg	Al	Si	Pb	K	Ca	Ba	Fe	Cu
% wt.	22.02	38.28	0.71	0.49	9.44	21.66	0.27	2.55	0.87	1.98	1.73	0
% at.	33.14	43.25	0.56	0.37	6.32	13.94	0.02	1.18	0.39	0.26	0.56	0

Table 19 The quantitative elemental composition of particle 6 from Figure 26.

6	C	O	Na	Mg	Al	Si	Pb	K	Ca	Ba	Fe	Cu
% wt.	19.54	36.97	0.7	0.64	7.2	13	0.92	1.23	0.31	1.72	17.49	0.28
% at.	31.91	45.32	0.6	0.52	5.24	9.08	0.09	0.62	0.15	0.25	6.14	0.09

Particles tagged on Figure 26 are less varied concerning composition, when compared to those depicted in Figure 25. Their elemental composition consists of the same elements. None of the particles differ significantly in composition. The biggest difference was found for particles 1 and 6, which contain small amounts of copper (the others do not). Moreover in their composition there is a higher contents of iron, which is around 17 % wt.. On the other hand, they are similar to particles 2, 3, 5 in terms of carbon and oxygen content but they show less quantity of silicon and aluminum than those mentioned. Particle 4, which differs from all the others is characterized by a higher carbon content.

5.4.2. Fly ash fraction with particle sizes under 63 µm.

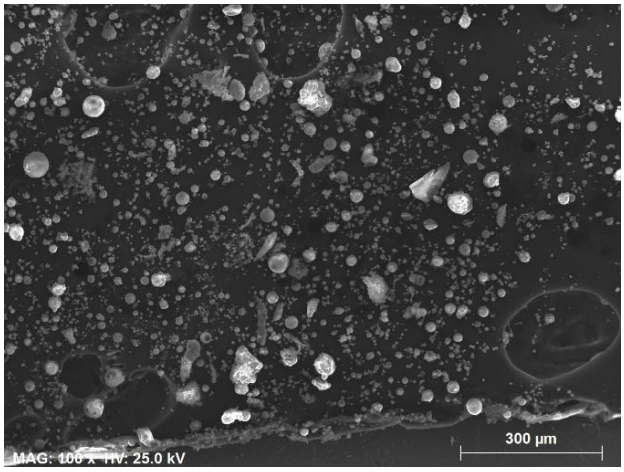

Figure 27 SEM image of FA, fraction under 63 µm, and 100x magnification.

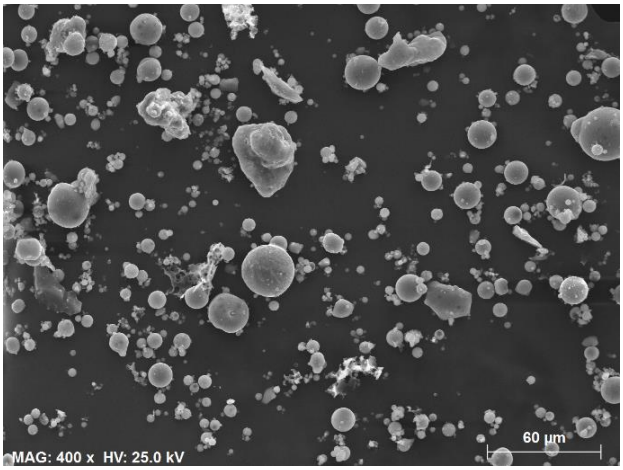

Figure 28 SEM image of FA, fraction under 63 µm, and 400x magnification.

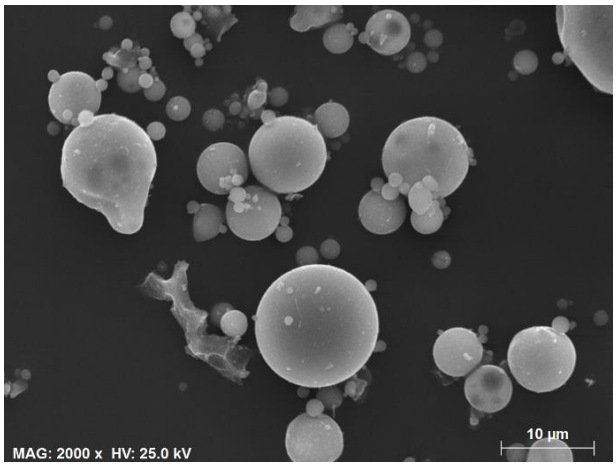

Figure 29 SEM image of FA, fraction under 63 µm, and 2000x magnification.

Figure 27, 28, 29, taken at different magnifications, evidence the dominant morphology for the smallest fly ash particles included in this fraction. Their characteristic shape is very regular and spherical. This morphology is typical of cenospheres. The particles diameter ranged from the limiting value 63 µm to spheres with a few µm diameter size.

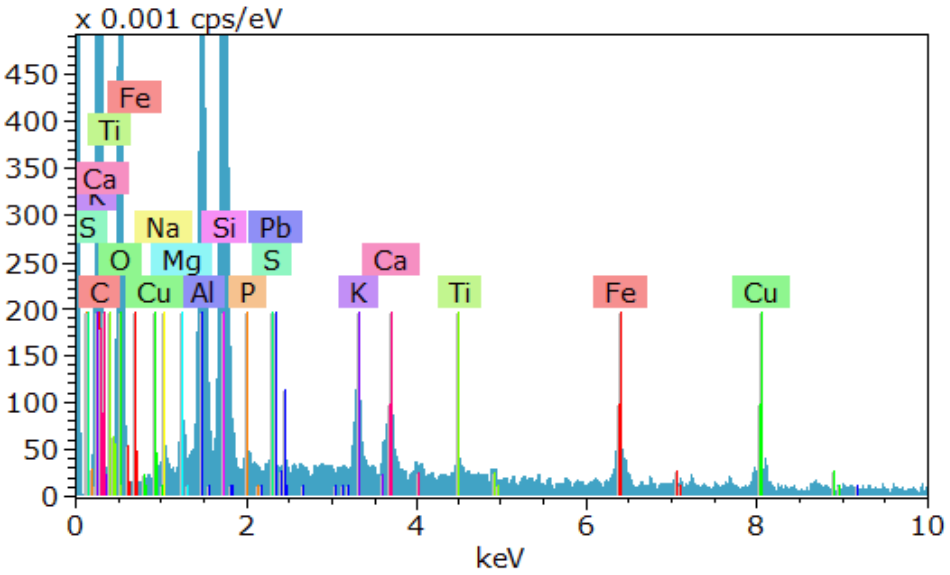

Figure 30 EDX spectrum of FA fraction under 63 µm.

Figure 30 shows the EDX spectrum of elements occurring in the fraction of fly ash with particle size under 63 µm. The atomic percentage (at.%) and weight percentage (wt.%) are depicted in Table 20 for the elements detected in the tested sample. There is a predominance of aluminum (25.42 % wt.) and silicon (42.30 % wt.) and relevant amounts of potassium, calcium, copper and iron.

Table 20 Weight and atomic percentage of detected elements in FA fraction under 63 µm.

1	Al	Ca	Cu	Fe	Mg	P	K	Si	Na	S	Ti
wt. %	25.42	4.94	5.59	4.47	2.57	3.22	5.93	42.30	2.93	1.36	1.27
at. %	28.58	3.74	2.67	2.43	3.20	3.16	4.60	45.68	3.86	1.28	0.81

5.4.3. Fly ash fraction with particle sizes between 63 – 100 µm.

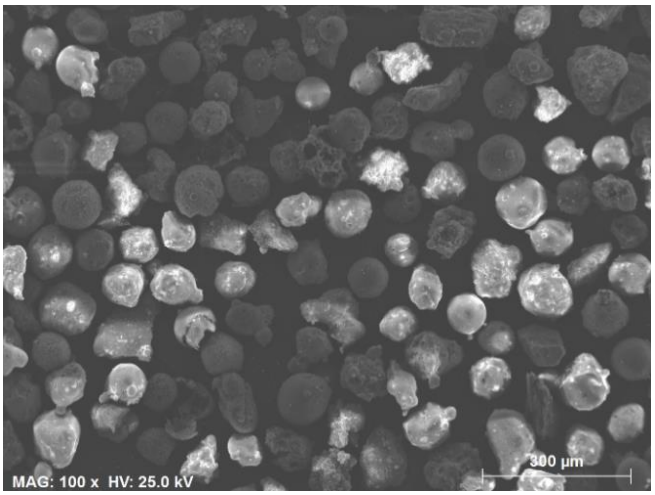

Figure 31 SEM image of FA, fraction between 63 - 100 µm, and 100x magnification.

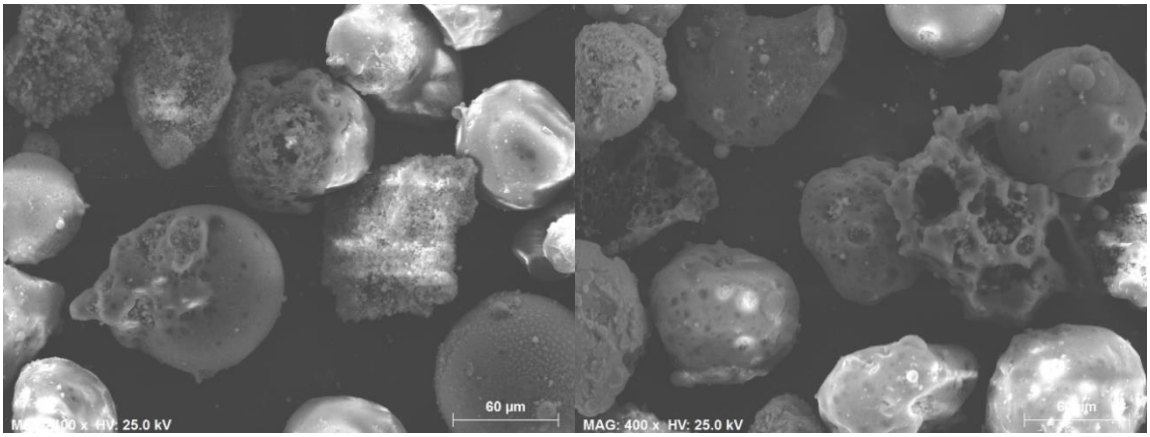

Figure 32 SEM images (a, b) of FA, fraction between 63 - 100 µm, and 400x magnification.

The fly ash fraction with particle size in range of 63 - 100 µm is quite distinct from those of the previous fraction. The particles are still spherical but their shapes are more irregular. In addition, spheres are not uniform and they are covered with smaller particles and irregular deposits.

Figure 33 shows the EDX spectrum of fly ash particles included in this fraction.

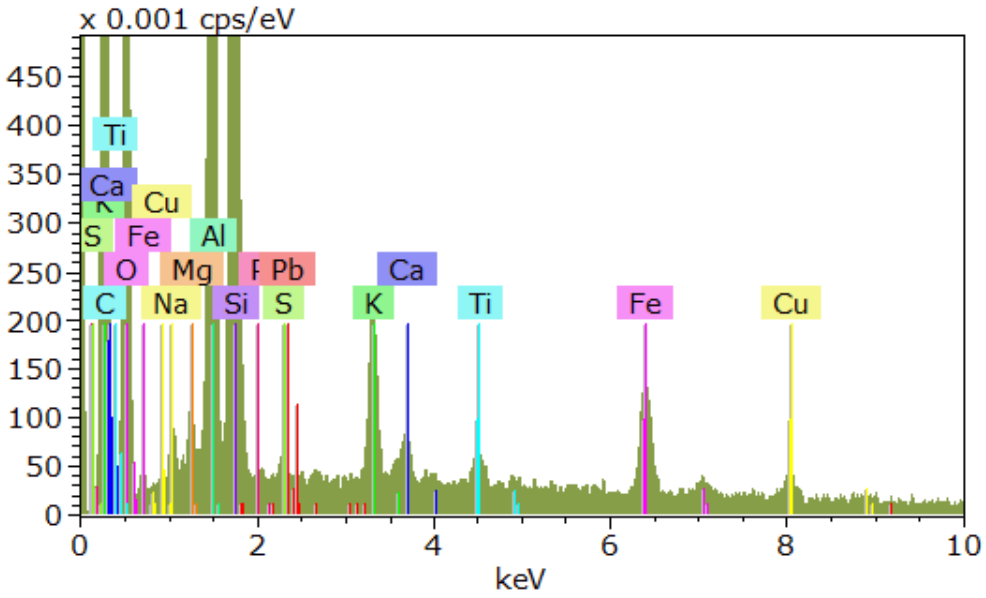

Figure 33 EDX spectrum of FA fraction between 63 - 100 µm.

Table 21 Weight and atomic percentage of detected elements in FA fraction between 63 – 100 µm.

2	Al.	Ca	Cu	Fe	Mg	P	K	Si	Na	S	Ti
wt. %	28.63	1.81	2.10	6.21	1.79	1.72	6.10	46.32	2.52	1.31	1.48
at. %	28.58	1.34	0.98	3.30	2.19	1.65	4.64	48.99	3.25	1.21	0.92

Moreover, Table 21 shows the composition for the detected elements. The dominant elements in this fraction are aluminum (28.63 % wt.) and silicon (46.32 %wt.), the next most numerous is iron (6.21 %t.), while sulphur is present with the smallest amount of (1.31 %wt.).

5.4.4. Fly ash fraction with particle sizes between 100 - 200 µm.

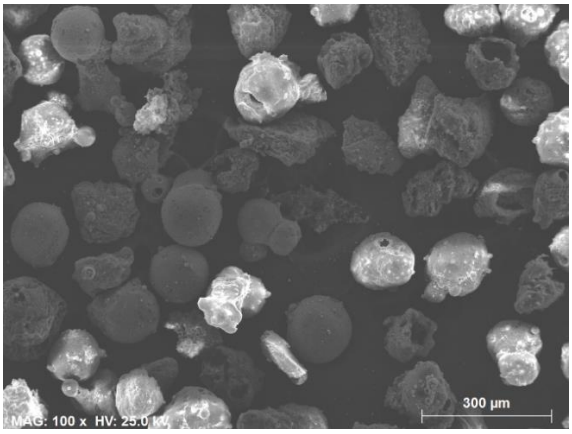

Figure 34 SEM image of FA, fraction between 100 - 200 µm, and 100x magnification.

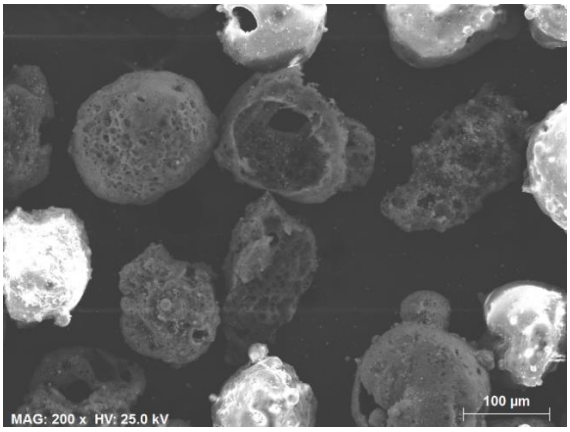

Figure 35 SEM image of FA, fraction between 100 - 200 µm, and 200x magnification.

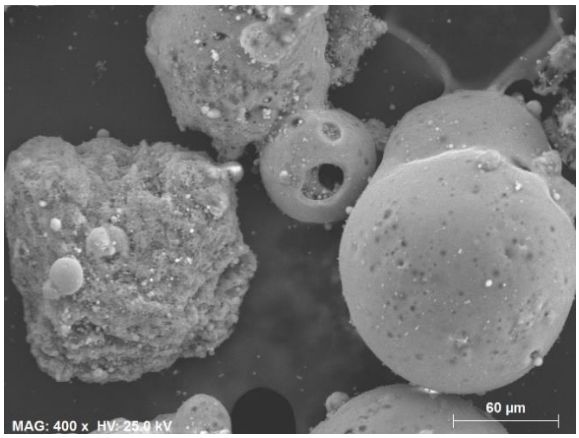

Figure 36 SEM image of FA, fraction between 100 - 200 µm, and 400x magnification.

Fly ash particles between 100 - 200 µm, are similar to the fraction 63 -100 µm. However the shapes of the particles are less uniform. The spheres are mixed with several particles, with irregular shapes, covered with smaller particles. There is a high probability to found magnetic spheres in this fraction, they are visible especially on Figure 36 (spheres covered with small particles over the surface). Also Figure 34 and 35 shows that there are several hollow cenospheres with holes in their shells.

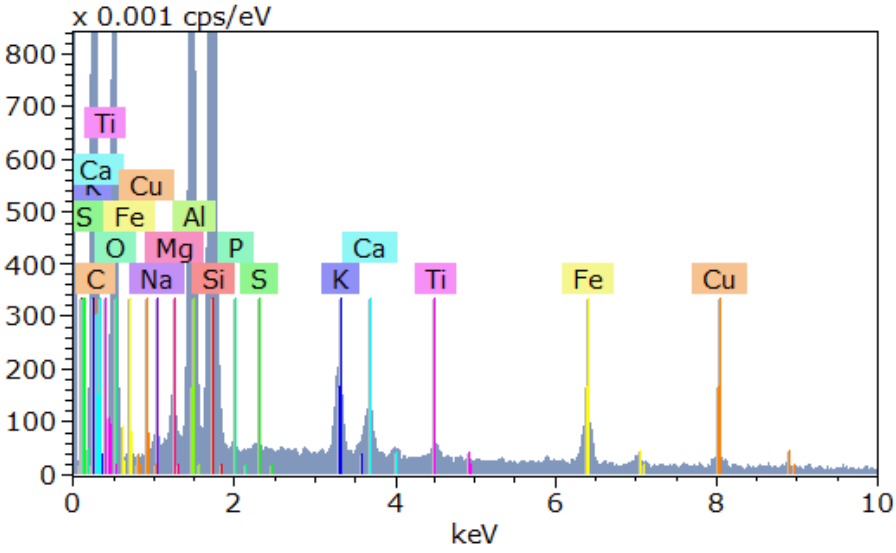

Figure 37 EDX spectrum of FA fraction between 100 - 200 µm.

Figure 37 shows the elemental composition of this fraction and Table 22 presents their quantitative profile using weight and atomic percentage.

Table 22 Weight and atomic percentage of detected elements in FA fraction between 100 -200 µm.

3	Al	Ca	Cu	Fe	Mg	P	K	Si	Na	S	Ti
wt. %	29.14	3.99	2.05	6.35	1.97	1.38	6.19	45.53	1.13	1.12	1.15
at. %	32.35	2.98	0.97	3.40	2.42	1.33	4.74	48.56	1.47	1.05	0.72

Table 22 shows that the most numerous element in this fraction is silicon (45.53 %wt.) the next is aluminum (29.14 %wt.) and then iron, potassium and calcium.

5.4.5. Fly ash fraction with particle sizes between 200 – 320 µm.

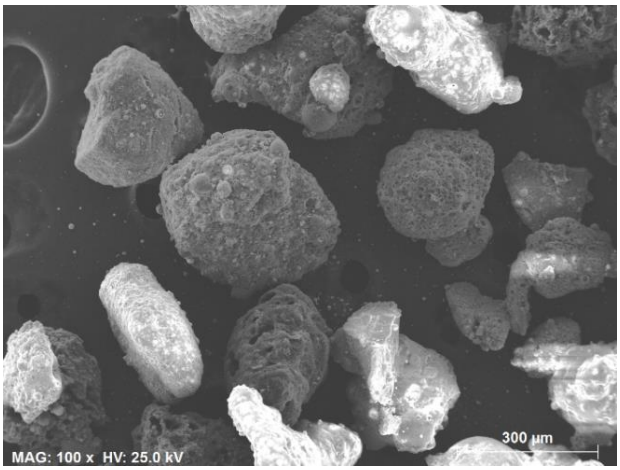

Figure 38 SEM image of FA, fraction between 200 – 320 µm, and 100x magnification.

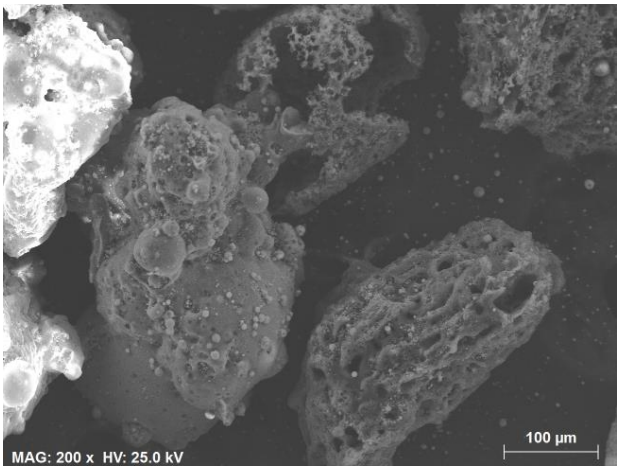

Figure 39 SEM image of FA, fraction between 200 – 320 µm, and 200x magnification.

The fraction which contains the particles in the range of 200 – 320 µm, reveals particles with different shapes (Figure 38, 39). Noticeable particles in this sample are irregular ones and there are no spherical particles. Irregular shapes evidence closed structures with several smaller particles covering their shells. As in the previous fraction it is very possible to find high content of particles with magnetic properties. Figure 40 represents EDX spectrum of this fraction.

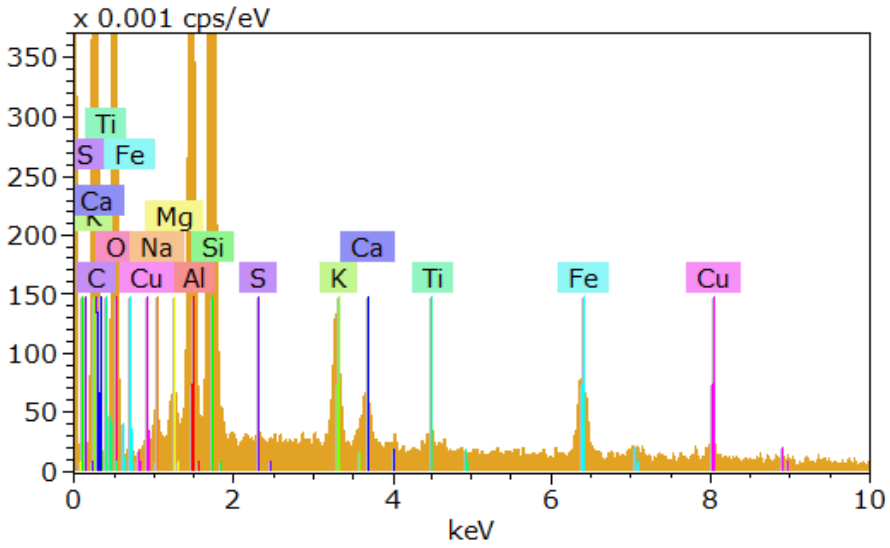

Figure 40 EDX spectrum of FA fraction between 200 - 320 µm.

Table 23 gathers the data about weight and atomic percentage of elements found in this fraction. As it was already mentioned Iron content (8.32 % wt.) responsible for magnetic properties is higher than in other fraction. However, quantitative comparison of elements detected in all fractions are presented in the following part of this work (Chapter 5.4.7).

Table 23 Weight and atomic percentage of detected elements in FA fraction between 200 - 320 µm.

4	Al	Ca	Cu	Fe	Mg	P	K	Si	Na	S	Ti
wt. %	27.38	3.24	2.93	8.32	1.82	0	7.12	45.77	1.99	0.40	1.04
at. %	30.77	2.45	1.40	4.52	2.27	0	5.52	49.41	2.62	0.38	0.66

5.4.6. Fly ash fraction with particle sizes above 320 µm.

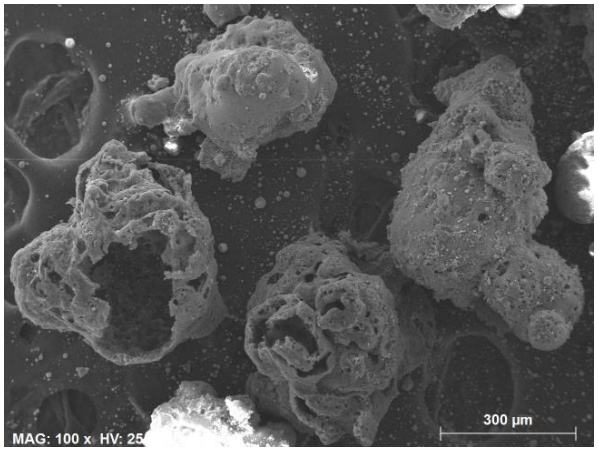

Figure 41 SEM image of FA, fraction above 320 µm, and 100x magnification.

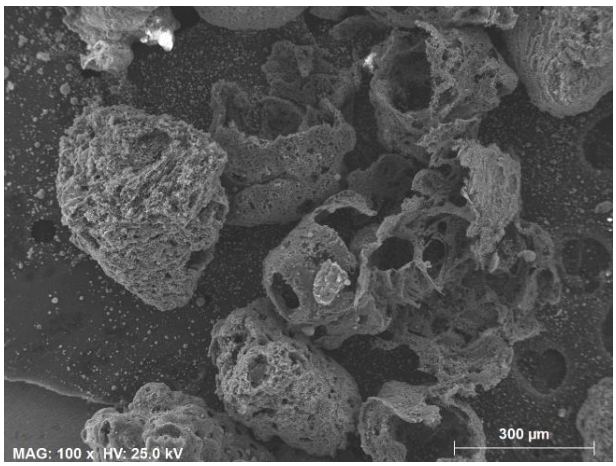

Figure 42 SEM image of FA, fraction above 320 µm, and 100x magnification.

The largest separated fraction is shown on Figure 41 and 42 and represents fly ash particles larger than 320 µm. These are the biggest particles possible to find in any fly ash. Particles included in this phase differ significantly from other fractions morphologically. Generally, this fraction consist only of big, extremely irregular, edgy-sharped particles that seems hollow in some cases.

Figure 43 depicts the EDX spectrum of elements detected in this fraction and Table 24 represents the quantitative profile of these elements.

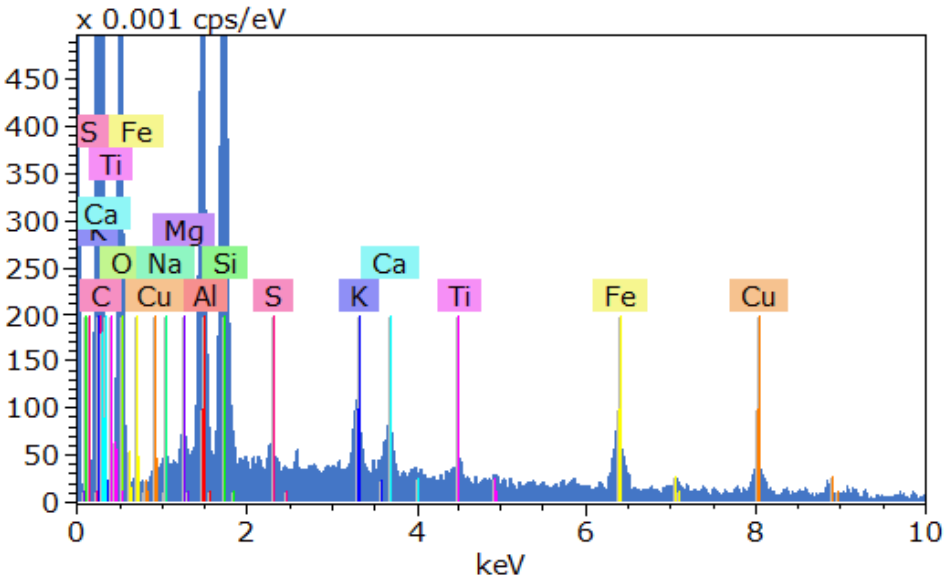

Figure 43 Figure 44 EDX spectrum of FA fraction above 320 µm.

Table 24 Weight and atomic percentage of detected elements in FA fraction above 320 µm.

5	Al	Ca	Cu	Fe	Mg	P	K	Si	Na	S	Ti
wt. %	27.57	4.90	7.87	10.33	1.58	0	5.60	36.19	1.57	2.15	2.24
at. %	32.63	3.91	3.96	5.91	2.07	0	4.58	41.15	2.18	2.14	1.49

Table 24 shows that in this fraction silicon (36.19 % wt.) and aluminum (27.57 % wt.) are still dominant but iron content (10.33 % wt.) as well as copper (7.87 % wt.) is much higher. Furthermore, in this fraction there is no phosphorus.

5.4.7. Comparison in terms of elemental composition

The EDX measurements obtained for each fraction can be compared, considering the content of the major and minor elements determined in the various fractions of fly ash. Therefore, the following tables show the compilation of atomic percentages for various elements detected (Table 25) and corresponding weight percentage (Table 26) for each fraction. To simplify, tables and graphs fractions will be numbered according to the size of particles as below:

Fraction 1 – Particle size under 63 µm,

Fraction 2 – Particle size between 63-100 µm,

Fraction 3 – Particle size between 100-200 µm,

Fraction 4 – Particles size between 200-320 µm,

Fraction 5 – Particles size above 320 µm.

Table 25 Summary of the elemental atomic composition, in percentage for each fraction from 1 to 5.

Fraction	Al	Ca	Cu	Fe	Mg	P	K	Si	Na	S	Ti
1	28.58	3.74	2.67	2.43	3.20	3.16	4.60	45.68	3.86	1.28	0.81
2	28.58	1.34	0.98	3.30	2.19	1.65	4.64	48.99	3.25	1.21	0.92
3	32.35	2.98	0.97	3.40	2.42	1.33	4.74	48.56	1.47	1.05	0.72
4	30.77	2.45	1.40	4.52	2.27	0	5.52	49.41	2.62	0.38	0.66
5	32.63	3.91	3.96	5.91	2.07	0	4.58	41.15	2.18	2.14	1.49

Table 26 Summary of the elemental weight composition, in percentage, for each fraction from 1 to 5.

Fraction	**Al**	**Ca**	**Cu**	**Fe**	**Mg**	**P**	**K**	**Si**	**Na**	**S**	**Ti**
1	25.42	4.94	5.59	4.47	2.57	3.22	5.93	42.30	2.93	1.36	1.27
2	28.63	1.81	2.10	6.21	1.79	1.72	6.10	46.32	2.52	1.31	1.48
3	29.14	3.99	2.05	6.35	1.97	1.38	6.19	45.53	1.13	1.12	1.15
4	27.38	3.24	2.93	8.32	1.82	0	7.12	45.77	1.99	0.40	1.04
5	27.57	4.90	7.87	10.33	1.58	0	5.60	36.19	1.57	2.15	2.24

For graphical representation only the weight composition was used. These plots represent only the elements that could be detected by the apparatus. Although the occurrence of minor or trace elements cannot be excluded, it was not possible to detect them by the apparatus (apart from Cu). Therefore, analyzed elements Al, Ca, Fe, Mg, P, K, Si, Na, S, Ti are all major elements that can occur in fly ash and Cu which represents trace elements.

Generally, in every fraction all the elements are present, except phosphorous which was not detected in fractions 4 and 5. This means that it occurs in fly ash particles with diameter less than or equal to 200 μm.

Aluminum and silicon are the two abundant elements which are fairly constant in all fractions (Figure 45). The aluminum content oscillates in the range of 25 to 30 % wt., while silicon is within the range 42 to 46 %wt. and slightly decreases in fraction 5, being equal to 36 % wt.. This result suggests that the particles are mainly composed of aluminosilicates [8].

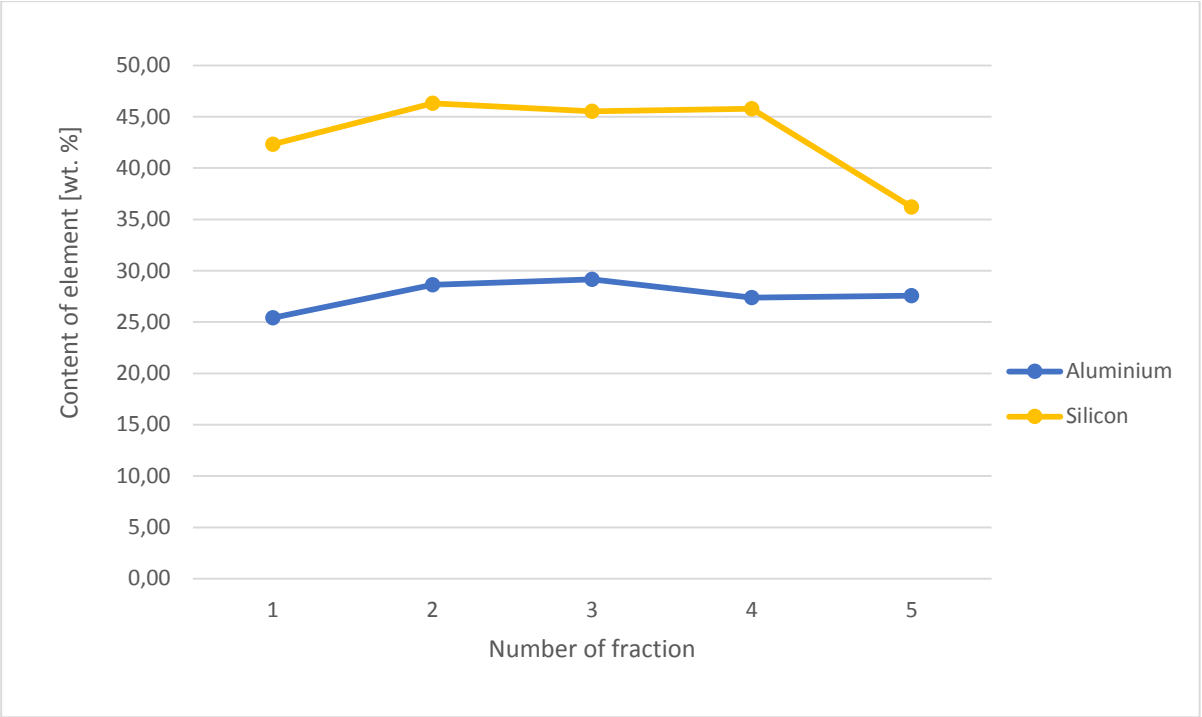

Figure 45 Aluminum and silicon distribution in all fractions of fly ash.

Another group of elements is characterized by a decreasing trend of their content as the particle size in the fraction increases (Figure 46). Thus, as the particle size increases, Mg and P contents decrease (indeed P vanishes for the two largest fractions). Sulphur also shows a decreasing trend, however, suddenly for the largest fraction it increases, probably because coal intended for combustion contained some amounts of sulphur which remains in unburnt carbon particles.

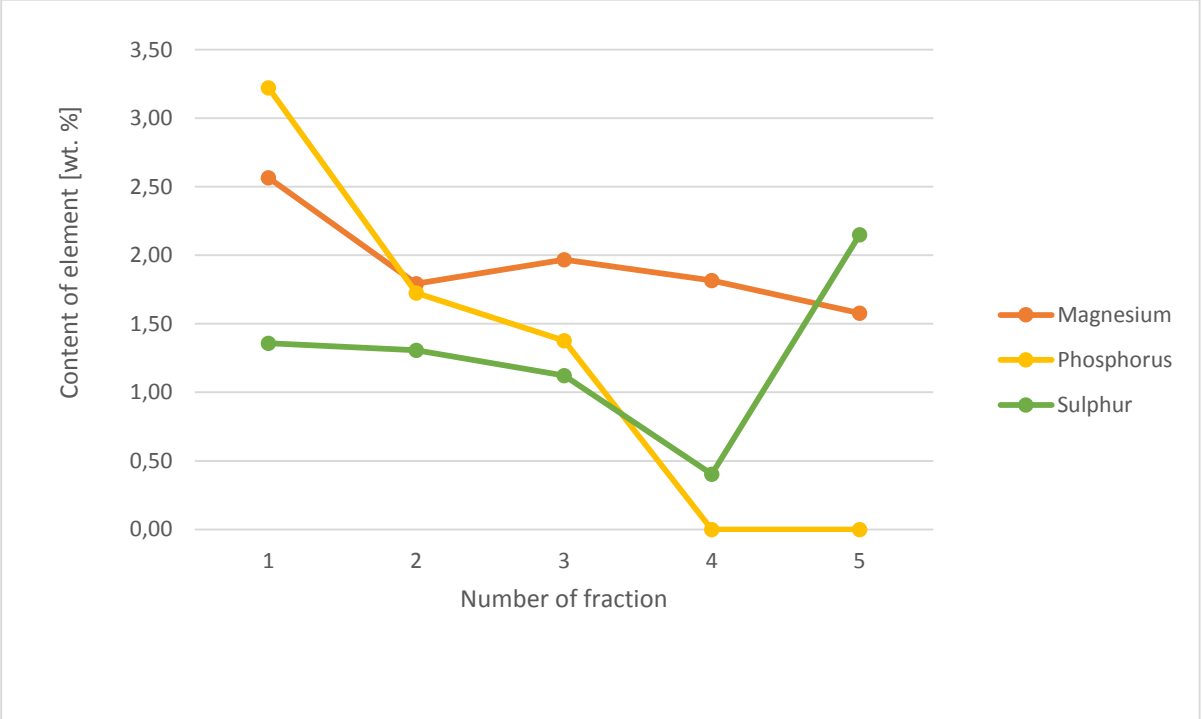

Figure 46 Magnesium, phosphorus and suplhur contents in all fractions of fly ash.

Phosphorus content gradually decreases from fraction 1 (above 3 % wt.) to fraction 2 (1.72 % wt.), fraction 3 (1.38 % wt.) and finally fractions 4 and 5 do not show phosphorous. Magnesium also shows a similar trend evolving from 2.56 % wt. in fraction 1 to 1.58 %wt. in fraction 5 (with some exception in fraction 2 where its content slightly increased). The next element which also shows this trend is sulphur. It decreases from 1.36% wt. in fraction 1 to 0.4 % wt. in fraction 4. In fraction 5 the content of sulphur increases again. Probably an higher content (2.15% wt.) of sulphur is related to dominant carbon in this fraction which also contains suplhur in their composition.

The content of Fe increases from fraction 1 (the smallest particles) to fraction 5 in which the particles are the largest. Iron content in fraction 1 is 4.47 % wt. in fraction 2 is 6.21 % wt. in fraction 3 is 6.35 % wt., in fraction 4 is 8.32 % and in fraction 5 is 10.33 % wt.. Fractions which are richer in iron show more marked higher magnetic properties.

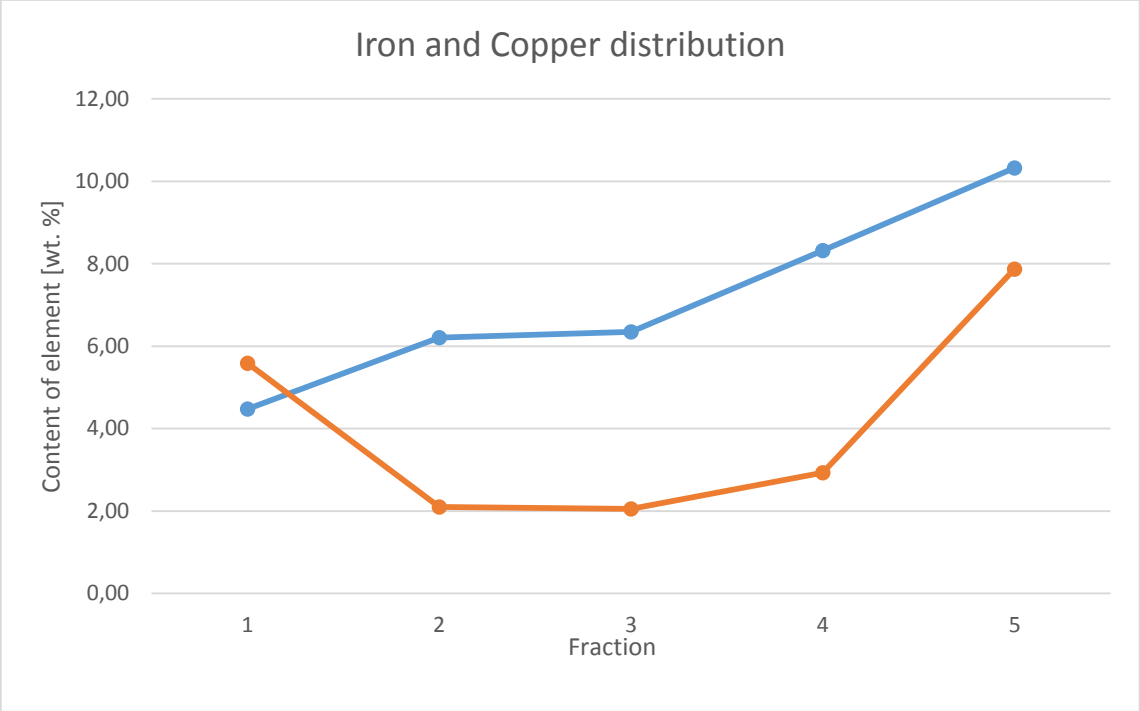

Figure 47 Iron and copper distribution in all fractions of fly ash.

The last element presented in figure 47 is copper that is present in all fractions. As it is shown on the figure there is no clear trend. However its content is higher in the smallest fraction as well as in the largest fraction. The lowest content of copper, around 2%, can be found in fraction 2 and 3.

5.5. XRD

X-ray diffraction (XRD) is an analytical technique that provides information about phases in crystalline materials, their structure and atomic spacing. XRD is a common method for finely ground and homogenized materials.

The technology working principle of X-ray diffraction is based on interference of X-rays with a sample of crystalline material. Monochromatic X-rays are produced by a cathode tube, filtered and concentrated directly into the sample. The most crucial condition, during the interaction of incident rays with the sample to produce constructive interference, is to satisfy the Bragg's Law. The Bragg's Law ($n\lambda=2d \sin\theta$) presents the dependency of wavelength of X-rays beam, diffraction angle and spacing in the lattice in the sample. When Bragg's Law is satisfied, the diffracted X-rays can be detected. A diffraction pattern is obtained from juxtaposition of diffracted intensity and the 2θ angles (figure 48) [58]. Materials, in which phases can be distinguished, can be characterized through diffraction pattern in terms of average weight of each phase, relatively, to their volume. Identification of phases is based on comparing the position of the three most frequent peaks in the pattern using patterns of pure substances specified in the JCPDS (Joint Committee on Powder Diffraction Standards) database.

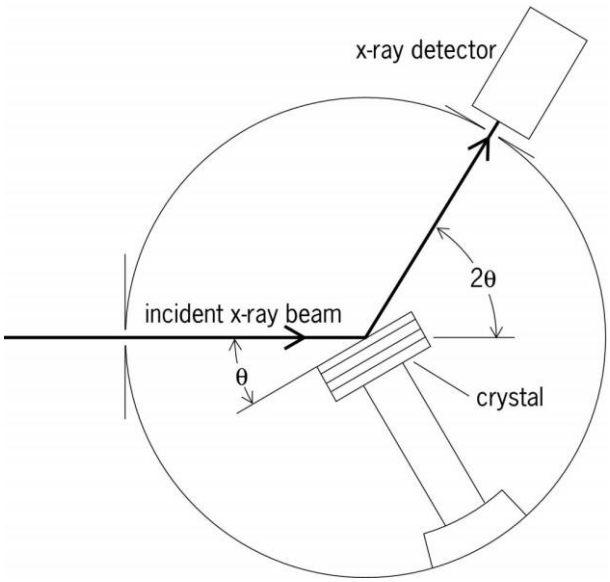

Figure 48 Schematic of X-rays diffraction [59].

X-ray diffraction of fly ash samples were performed in the 10-110 deg range under the CuK_α radiation, using PANalytical Empyrean diffractometer. The tests were carried out in the X-Ray diffraction laboratory at University of Science and Technology in Kraków.

The XDR patterns for different fractions are presented in figures 49 – 53. The presentation of the results, obtained for each fraction, starts from the smallest fraction up to the largest one.

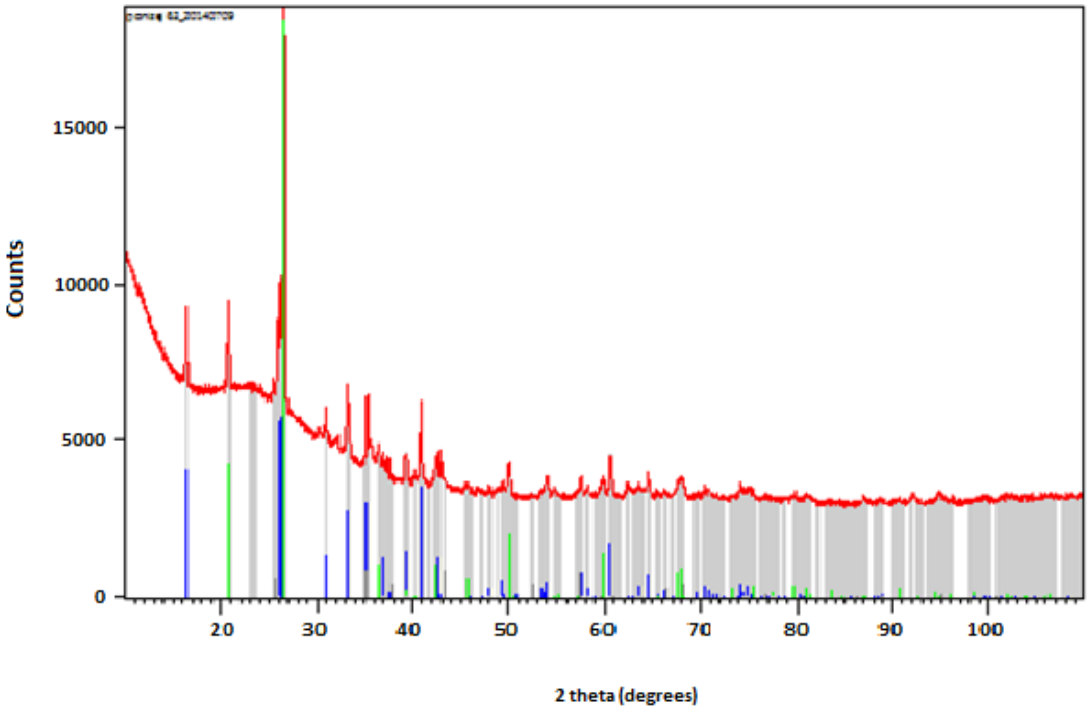

Figure 49 XRD pattern of FA fraction under 63 μm.

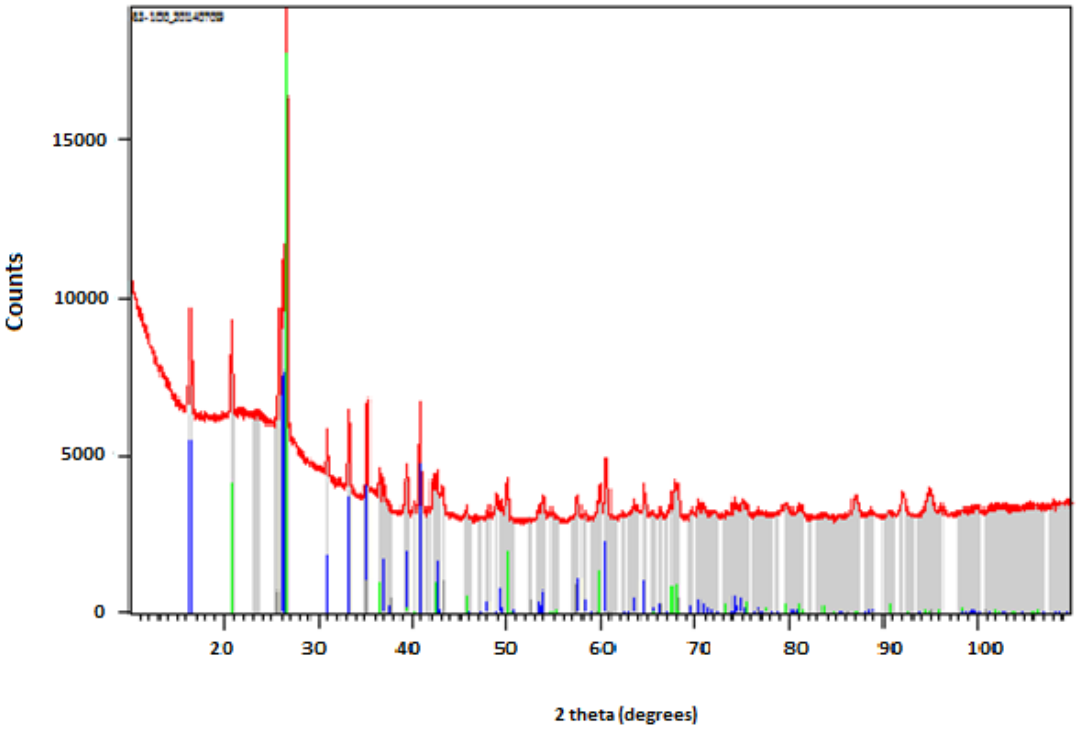

Figure 50 XRD pattern of FA fraction 63-100 μm.

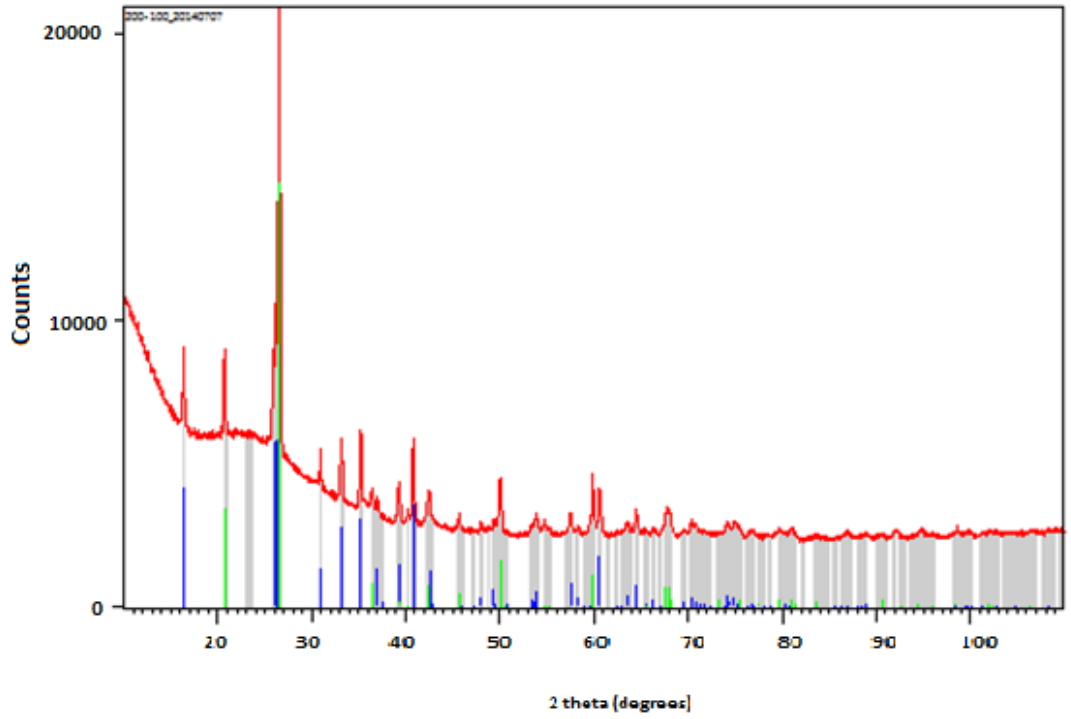

Figure 51 XRD pattern of FA fraction 100-200 µm.

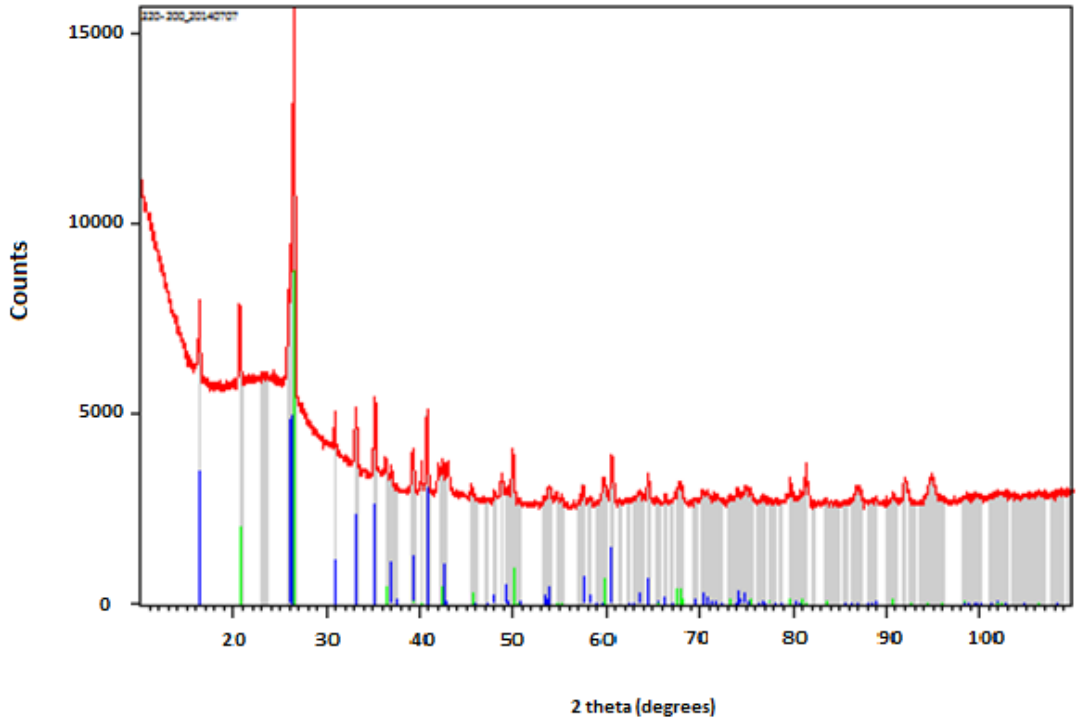

Figure 52 XRD pattern of FA fraction 200-320 µm.

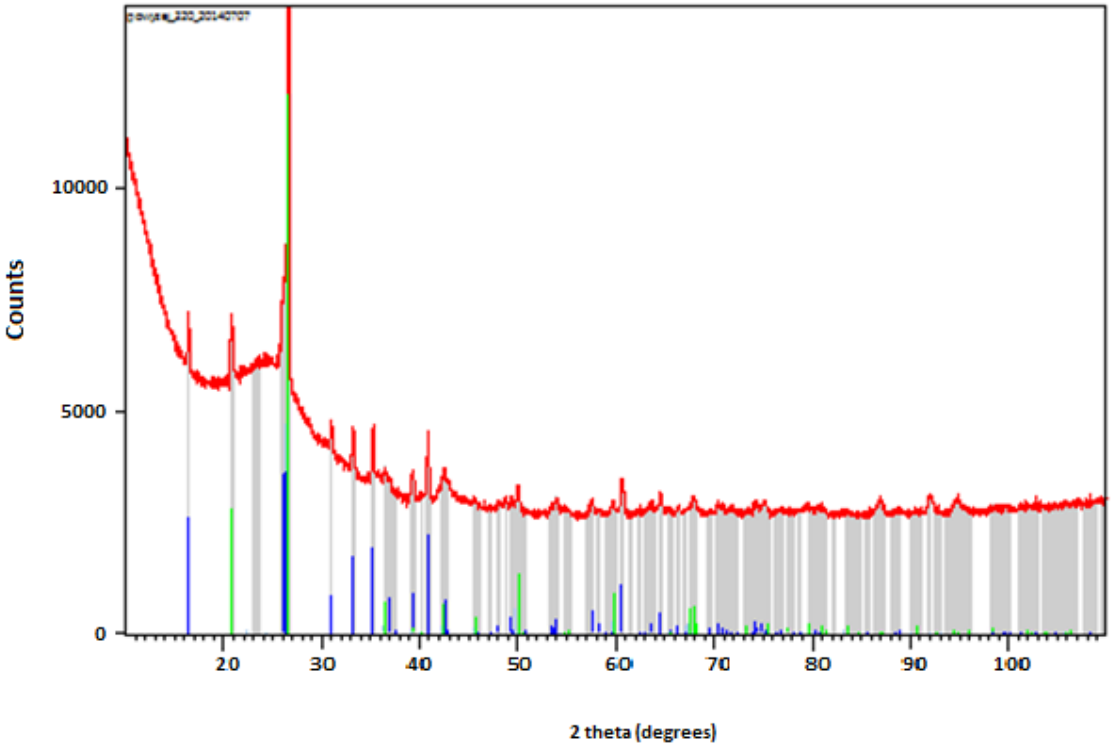

Figure 53 XRD pattern of FA fraction above 320 µm.

Table 27 Amounts of compounds in each fraction.

	Compound in % wt.		
Fraction	Aluminum Silicon Oxide	Silicon Oxide	Aluminum Oxide
Under 63 µm	64	29	7
63 - 100 µm	70.7	23.2	6.1
100 – 200 µm	65	24	11
200 – 320 µm	71	18	11
Above 320 µm	61.4	29.7	8.9

Moreover, based on XRD results different phases were found in the samples. Aluminum silicon oxide, silicon oxide and aluminum oxide were detected in every fraction but in different quantity. Table 27 shows the proportion of weight ratio of phases for each fraction separately. While Figure 54 graphically demonstrates the distribution of those three compounds.

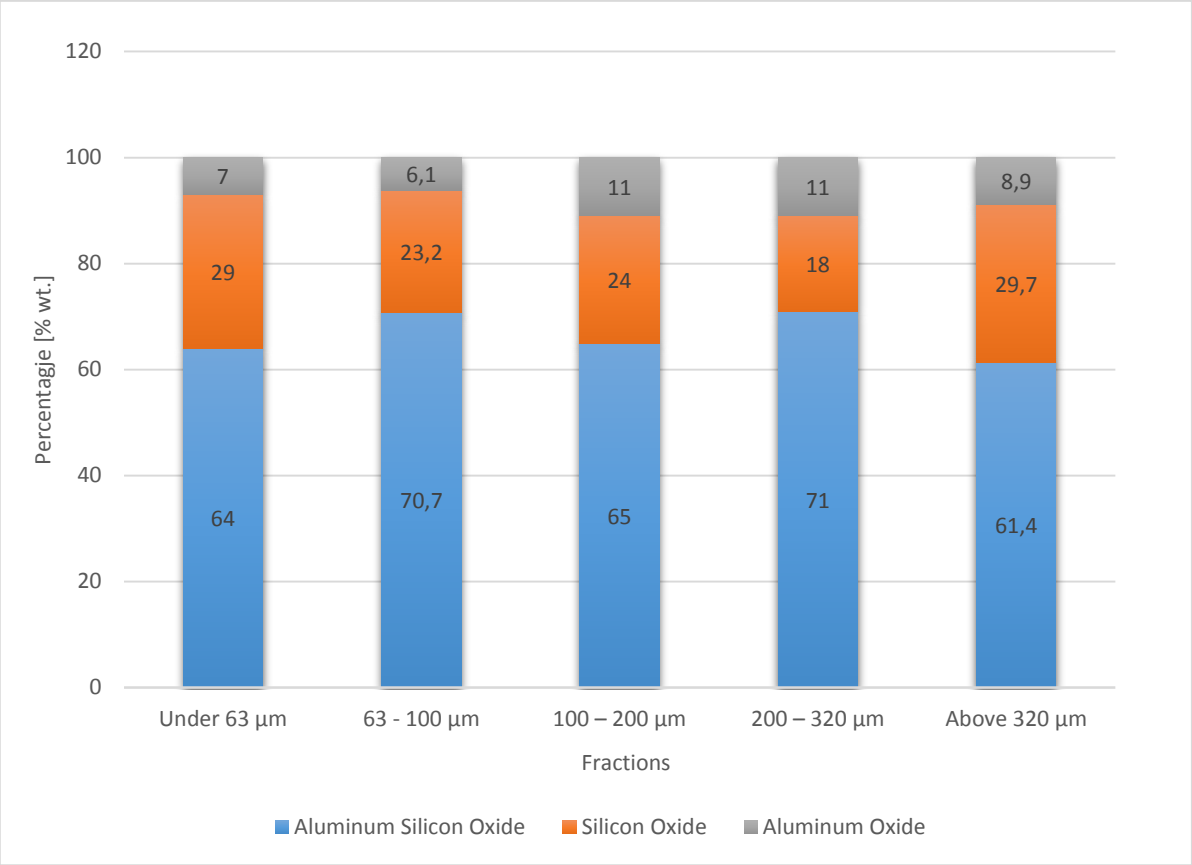

Figure 54 Distribution of different phases in fractions of fly ash.

From the results, it is possible to notice all fractions, in terms of their phase compositions, were found to be similar. The only difference between them is their weight proportions of compounds. The most abundant compound in all fractions is aluminum silicon oxide, which content ranges from 61.4 % wt. (in the fraction above 320 µm) to 71 % wt. (in the fraction with particles sizes from 200 – 320 µm). The second most frequent compound is silicon oxide. Its composition in fly ash fractions oscillates from 18 % wt. (in fraction 200 – 320 µm) up to 29.7 % wt. (in fraction above 320 µm). The content of silicon oxide is also high (29 % wt.) in the smallest fraction of fly ash with particles under 63 µm. The fraction with particles between 63 -100 µm and 100 – 200 µm indicates, 23.2 % wt. and 24 % wt. content of silicon oxide, respectively. The last compound is aluminum oxide, its content is in range between 6.1% wt. (in fraction 63 – 100 µm) up to 11 % wt. (in fractions 100 – 200 µm and 200 - 300 µm). Remaining values of aluminum oxide contents are as follows: 7% wt. in fraction under 63 µm and 8.9 % wt. in fraction above 320 µm.

6. Conclusions

Fly ash from coal combustion has been studied to obtain detailed information about its characterization. For this purpose, fly ash samples were separated into five different fractions with various particles sizes ranges (above 320 μm, 320-200 μm, 200-100 μm,100-63 μm and under 63 μm). Thus, it was possible to compare physical properties of the fractions and investigate them in terms of their morphology, elemental composition and phase composition.

Results clearly show that various fractions of fly ash differ from each other. In general they differ visually in terms of their color. The biggest fraction includes very dark, black particles and then the color of the particles becomes clearer, up to light grey, in the smallest fraction. This is due to higher content of unburnt carbon in the thickest fractions which is not so numerous in lower fractions.

Moreover the Malvern Mastersizer 2000 measurements provide details about the quantitative profile of fly ash. Fly ash particles start from 2 μm and vanish when they gain 340 μm. The dominant sizes of fly ash particles were in range between 60-200 μm with the maximum peak at 100 μm. However the most abundant particles were in range from 2 μm to 60 μm which cover more than 60% wt. of fly ash sample.

Results obtained from scanning electron microscope (SEM) shows the morphological variation present in the different fractions of fly ash. It was proved that fly ash particles with diameter size under 63 μm (the smallest fraction) significantly vary from fly ash particles with diameter size above 320 μm (the biggest fraction). This is due to different formation in each fraction. In the smallest fraction the dominant are cenospheres which characterize with regular spherical shape while in the biggest fraction prevail formation is unburnt carbon with extremely irregular and jagged shapes of particles. Furthermore remaining fractions also vary from each other. The differences are analogous, in the fraction with particles in ranges between 63-100 μm there is a mixture of predominance spherical particles (cenospheres) with irregular particles, then with each fraction the amount of irregular particles successively increases up to mentioned fraction (above 320 μm) where they occur exclusively.

Moreover the elemental composition, received from electron dispersive X-ray spectroscopy (EDX), of the fly ash vary within the fractions. The dominant elements, which are silicon and aluminum show fairly constant amounts in all fractions. For other detected elements in general it is possible to find a trend. Phosphorous, magnesium and sulphur show a decreasing trend from the smallest fraction to the largest. Iron and copper were elements, for which contents increased from the smallest fraction to the largest. The remaining elements did not revealed any particular trend.

The last survey, which was X-ray diffraction (XRD), provided information of the phase composition. Results give an indicative view for fly ash phase composition which consist only of three phases (aluminum silicon oxide, silicon oxide and aluminum oxide). The most abundant phase is composed of aluminum silicon oxide, the second largest is silicon oxide and the least numerous aluminum oxide. The study showed that the individual fractions are not significantly different in their phase composition.

7. Future work

The results obtained in the present work on fly ash from coal combustion and their characterization led to several proposals for future work:

- To obtain separated fractions, with diameter size smaller than 63 μm, and to search for a more precise dependency in terms of elemental composition as well as morphological changes.

- To perform more detailed studies using modern quantitative techniques for example Inductively Coupled Plasma (ICP) that may detect and quantify elements down to the ppm range.

- To use Raman Spectroscopy to obtain structural information and to detail the chemical composition.

- To release guidelines concerning fly ash applications.

References

[1] L. C. Ram, R. E. Masto, *An appraisal of the potential use of fly ash for reclaiming coal mine spoil,* Journal of Environmental Management, (2010), 91(3), pp 603–617

[2] National Energy Technology Laboratory. *Clean coal technology: Coal utilization by-products. Washington*, DC: Department of Energy Office of Fossil Energy; (2006), Report no. 24.

[3] Coal classification 2014, Received from The Engineering Tool Box, http://www.engineeringtoolbox.com/classification-coal-d_164.html

[4] L. D. Smoot, *Fundamentals for coal combustion for coal and efficient use,* Coal Science and Technology, Elsevier, (1993), 20

[5] S. A. Benson , P. L. Holm, *Comparison of inorganics in three low-rank coals, Ind. Eng. Chem. Prod. Res. Dev.*, (1985), 24 (1), pp 145–149

[6] M. L. Jones, D. P. Kalmanovitch, E. N. Steadman, C. J. Zygarlicke, S. A. Benson *Application of SEM Techniques to the Characterization of Coal and Coal Ash Products,* Advances in Coal Spectroscopy Modern Analytical Chemistry, (1992), pp 1-27

[7] N. Gamage, K. Liyanage, S. Fragomeni, S. Setunge *Overview of different types of fly ash and their use as a building and Construction materia*l, Proceedings of the International Conference of Structural Engineering, Construction and Management Kandy, Sri Lanka, (2011)

[8] M. Ahmaruzzaman, *A review on the utilization of fly ash*, Department of Chemistry, National Institute of Technology Silchar, Progress in Energy and Combustion Science 36 (2010), pp 327–363

[9] D. K. Szponder, K.Trybalski, *Określanie właściwości popiołów lotnych przy użyciu różnych metod i urządzeń badawczych*, Górnictwo i Geoinżynieria, (2009), 287

[10] D. P. Mishra, S. K. Das, *A study of physic-chemical and mineralogical properties of Talcher coal fly ash for stowing in underground coal mines*, Minerals Characterization, (2010), 63 (11), pp 1252-1259

[11] J. Małolepszy, E. Tkaczewska, *Wpływ frakcji ziarnowej krzemionkowych popiołów lotnych na proces hydratacji i właściwości cementu*, V Konferencja Naukowo-Techniczna, (2007), pp 331-339

[12] B. Pieńkowski, *Ceramika z popiołów [cz.1],* Ceramika Budowlana i Silikaty, (1999), pp 25-27

[13] M. A. Glinicki, M. Zieliński, *Rozmieszczenie porów powietrznych w betonie z dodatkiem fluidalnego popiołu lotnego*, Cement Wapno Beton, (2007), 12/74(3), pp 133-138

[14] J. Kabała, J. Listkiewicz, *Wpływ stabilizacji składu chemicznego, fizycznego i ilościowego ubocznych produktów spalania węgla i odsiarczania spalin węgla z kotłów fluidalnych na możliwość ich gospodarczego wykorzystania*, Fluidalne spalanie węgla w energetyce, (2004), pp 124-130

[15] K. Galos, A. Uliasz-Bocheńczyk, *Źródła i użytkowanie popiołów lotnych ze spalania węgli w Polsce*, Gospodarka surowcami mineralnymi, (2005), 21(1)

[16] J. Małolepszy, W. Wons, *Wpływ właściwości fizykochemicznych popiołów lotnych z węgla kamiennego na spiekalność wyrobów z ceramiki budowlanej*, V Konferencja Naukowo-Techniczna "Zagadnienia Materiałowe w Inżynierii Lądowej", (2007), pp 340-348

[17] Y. J. Feng, F. Li, X. L. Wang, X. M. Liu, L. Zhang, *Principal Chemical Properties of Artificial Soil Composed of Fly Ash and Furfural Residue*, Pedosphere, (2006), 16(5), pp 668-672

[18] Z. Giergiczny, *Popiół lotny aktywnym składnikiem cementu*, IV Sympozjum Naukowo-Techniczne Górażdże Cement: Reologia w technologii betonu, (2002), pp 5-15

[19] K. Kasprzyk, P. Pietrykowski, *Wykorzystanie popiołów lotnych w gospodarce,* Zakład Spalania i Detonacji, (2007)

[20] A. Gonet, S. Stryczek, R. Wojciechowski, *Wytrzymałość na ściskanie zaczynów cementowo-iłowych z dodatkiem popiołu fluidalnego „Żerań"*, Wiertnictwo Nafta Gaz, (2005), 22 (2)

[21] S. Bastian, *Betony konstrukcyjne z popiołem lotnym*, Warszwa: Arkady, (1980)

[22] V. C. Pandey, N. Singh, *Impact of fly ash incorporation in soil systems, Agriculture, Ecosystem and Environment*, (2010), 136, pp 16-27

[23] J. J. Hycnar, *EUROCOALASH – weryfikacja popiołów ze spalania węgla*, Energetyka, (2009), 62(1), pp 48-53

[24] M. Mazurkiewicz, Z. Piotrowski, Propozycja unormowania badań będących podstawą dopuszczenia odpadów drobnofrakcyjnych do deponowania w pustkach podziemnych, Bezpieczeństwo Pracy i Pchrona Środowiska w Górnictwie, (1995), pp 13-17

[25] E. Tkaczewska, J. Małolepszy, Badania składu fazowego i struktury szkła we frakcjonowanych krzemionkowych popiołach lotnych, Problemy naukowo-badawcze budownictwa, (2008), 5, pp 411-418

[26] E. Gürlich, *Stan szklisty*, Kraków wydawnictwo AGH, (1989)

[27] W. P. Linak, J. O.L. Wendt,*Trace metal transformation mechanisms during coal combustion,* Fuel Processing Technology, (1994), 39, pp 173–198

[28] C. Rosik-Dulewska*, Podstawy gospodarki odpadami*, Warszawa: PWN, (2005)

[29] P. Basu, *Combustion and Gasification in Fluidized Beds*, Taylor & Francis Group, (2006)

[30] P. R. Salomon, T. H. Fletcher, R. J. Pubmire, *Progress in coal pyrolysis*, (1993), Fuel 72(5), pp 587-597

[31] Z. Bis, *Kotły fluidalne: teoria I praktyka*, Częstochowa: Wydawnictwo Politechniki Częstochowskiej, (2010)

[32] T. Trybuś, *Fluidalne spalanie paliw jako metoda ograniczenia emisji dwutlenku siarki I tlenków azotu,* Ochrona Środowiska, (1995), pp 15-18

[32] P. Sulovsk, *Mineralogy and chemistry of conventional and fluidised bed coal ashes*, Department of Mineralogy, Petrology and Geochemistry, Masaryk University, Brno, Czech Republic, Bulletin of the Czech Geological Survey, (2002), 77(1), pp 1–11,

[33] http://www.neundorfer.com/knowledge_base/electrostatic_precipitators.aspx [accessed on 28th September 2014]

[34]http://yosemite.epa.gov/oaqps/eogtrain.nsf/fabbfcfe2fc93dac85256afe00483cc4/bbd8958eb8fbeeea85256da3005cc39d/$FILE/SI%20445_10.pdf [accessed on 28th September 2014]

[35] W. P. Linak, J. O.L. Wendt, *Trace metal transformation mechanisms during coal combustion,* Fuel Processing Technology, (1994), 39, pp 173–198

[36] R.S. Blissett, N.A. Rowson, *A review of the multi-component utilisation of coal fly ash*, (2012), Fuel 97, pp 1–23

[37] N.L. Ukwattage, P.G. Ranjith, M. Bouazza *The use of coal combustion fly ash as a soil amendment in agricultural lands (with comments on its potential to improve food security and sequester carbon,)*, (2013), Fuel 109, pp 400–408

[38] S. M. Shaheen, P. S. Hooda, C. D. Tsadilas *Opportunities and challenges in the use of coal fly ash for soilimprovements - A review,* Journal of Environmental Management (2014), 145, pp 249-267

[39] G. Yilmaz, *Structural characterization of glass–ceramics made from fly ash containing SiO2–Al2O3–Fe2O3–CaO and analysis by FT-IR–XRD–SEM methods,* Journal of Molecular Structure, (07/2012), pp 37–42

[40] J. E. Oh, Y. Jun, Y. Jeong, *Characterization of geopolymers from compositionally and physically different Class F fly ashes,* Cement and Concrete Composites, (2014), 50, pp 16-26

[41] Image adapted from *The Future of Fly Ash Use in Concrete*, (11/2013),

http://precast.org/2013/11/the-future-of-fly-ash-use-concrete/ [accessed on 24th October 2014]

[42] J. Tomeczek, H. Palugniok*, Kinetics of mineral matter transformation during coal combustion* (2002), Fuel, 81 (10), pp 1251–1258

[43] M. Jedrusik, A. Świerczok, The influence of fly ash physical and chemical properties on electrostatic precipitation process, Journal of Electrostatics (07/2009), 67, pp 105–109

[44] S. H. Leea, E. Sakaib, M. Daimonb, W. K. Bangc, *Characterization of fly ash directly collected from electrostatic precipitator,* Cement and Concrete Research (1999), 29, pp 1791–1797

[45] http://www.concreteanswers.org/CIPs/CIP30.htm [accessed on 20th October 2014]

[46] Y. Fan, F. Zhang, J. Zhua, Z. Liu, *Effective utilization of waste ash from MSW and coal co-combustion power plant—Zeolite synthesis*, Journal of Hazardous Materials (2008), 153, pp 382–388

[47] American Society for Testing and Materials website: http://www.astm.org/Standards/C618.htm

[48] M. J. Dudas, C. J. Warren, *Submicroscopic structure and characteristics of intermediate- calcium fly ashes,* Symposium Proceedings of Material Research Society, (1988), 113, pp 309-316

[49] J. Kucowski, D. Laudyn, M. Przekwas, *Energetyka a środowisko*, Warszawa: Wydawnictwo Naukowo-Techniczne, (1997)

[50] J. M. K. O'Keefe, A. Bechtel, K. Christanis, S. Dai, W. A. DiMichele, C. F.Eble, J. S. Esterle, M. Mastalerz, A. L. Raymond, B. V. Valentim, N. J. Wagner, C. R. Ward, James C. Hower, *On the fundamental difference between coal rank and coal type*, International Journal of Coal Geology (2013), 118, pp 58-87,

[51] S. Wang, *Application of Solid Ash Based Catalysts in Heterogeneous Catalysis, Environ. Sci. Technol., (*2008), 42 (19), pp 7055–7063

[52] Website of Malvern Company:

http://www.malvern.com/en/products/product-range/mastersizer-range/mastersizer-2000/default.aspx

[accessed on 10th November 2014]

[53] http://www.atomikateknik.com/pdf/Mastersizer2000.pdf [accessed on 10th November 2014]

[54] http://micron.ucr.edu/public/manuals/Sem-intro.pdf [accessed on 24th October 2014]

[55] http://serc.carleton.edu/research_education/geochemsheets/techniques/SEM.html [accessed on 24th October 2014]

[56] http://www.surfacesciencewestern.com/analytical-services/scanning-electron-microscopy-coupled-with-energy-dispersive-x-ray-semedx-spectroscopy/ [accessed on 22nd October 2014]

[57] M. R. Martinez-Taranoza, D. A. Spears, *The fate of trace elements and bulk minerals in pulverized coal combustion in power station*, Fuel Processing Technology (1997), 47, pp 79- 92

[58] http://serc.carleton.edu/research_education/geochemsheets/techniques/XRD.html [accessed on 24th October 2014]

[59] http://encyclopedia2.thefreedictionary.com/x-ray+diffraction [accessed on 24th October 2014]